

Synthesis, Characterisation and Evaluation of In Vitro Toxicity in Hepatocytes of Linear Polyesters with Varied Aromatic and Aliphatic Co-monomers

Deepak Kakde^a, Leigh G. Powell^b, Kuldeep K Bansal^a, Steve Howdle^c, Derek Irvine^d, Giuseppe Mantovani^a, Gavin Millar^b, Lea Ann Dailey^e, Vicki Stone^b, Helinor J Johnston^{b} and Cameron Alexander^{a*}*

^a School of Pharmacy, University of Nottingham, University Park, Nottingham, NG72RD, UK. e-mail: cameron.alexander@nottingham.ac.uk

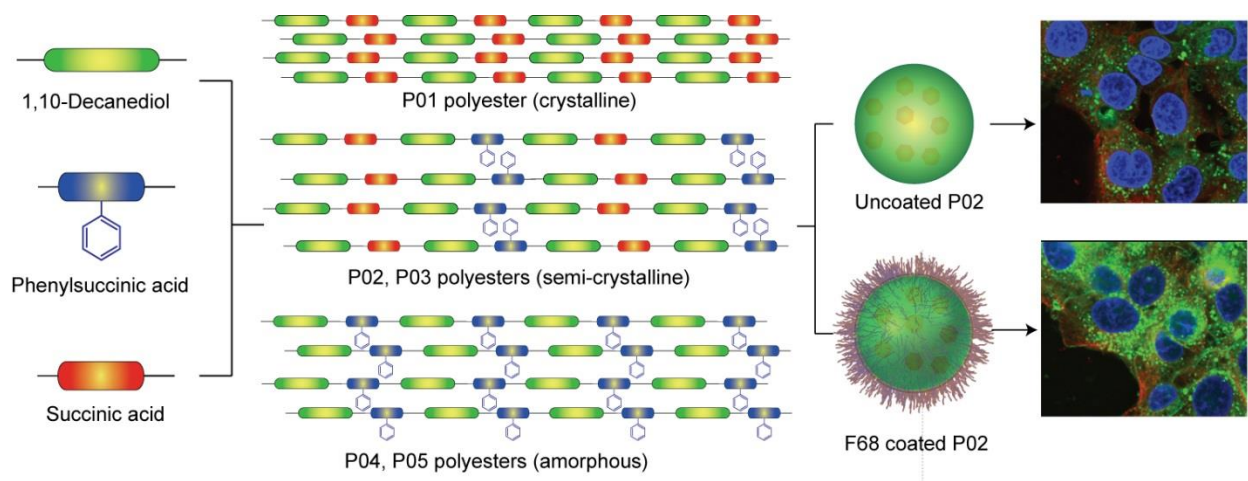
^b School of Life Sciences, Nano Safety Research Group, Heriot-Watt University, Edinburgh, EH14 4AS, UK. E-mail: H.Johnston@hw.ac.uk.

^c School of Chemistry, University of Nottingham, University Park, Nottingham NG72RD, UK

^d Department of Chemical and Environmental, Faculty of Engineering, Engineering, University of Nottingham, University Park, Nottingham, NG7 2RD, UK

^e Institute of Pharmaceutical Technology and Biopharmaceutics, Martin-Luther-University Halle-Wittenberg, Wolfgang-Langenbeck-Str. 4, D - 06120 Halle / Saale

ABSTRACT



Polyesters are extensively used in drug delivery because of their controllable biodegradation properties and perceived favourable cytocompatibility. However, new ester-based materials are continually being sought which can be produced from readily accessible monomers, which can be tuned for drug encapsulation and which retain good cellular compatibilities. In this study, 5 polyesters of similar molar mass were synthesized by reacting 1,10-decanediol with different ratios of succinic acid/phenylsuccinic acid and the effect of the phenyl side-chain group addition on polymer properties relevant to drug delivery was investigated. A polymer with a 70/30 ratio of succinic acid and phenylsuccinic acid was selected based on its ability to encapsulate a model dye in nanoparticle (NP) formulations, and was found to be slowly degradable in phosphate buffered saline (PBS) but more rapidly degraded in the presence of a lipase. The compatibility of NP formulations of this polymer either with or without a Pluronic F68 stabilizing coating was assessed *in vitro* using the C3A hepatocyte cell line. Cell viability was assessed, at NP concentrations ranging from 4.68 - 300 $\mu\text{g}/\text{mL}$ 24 h post exposure, using the Alamar Blue, CDFA and Neutral Red assays.

C3A cells internalised both coated and uncoated polyester NPs to a similar extent, with uptake observed to increase over time (10 - 1440 min). Although cell viability was greater than 80% at the concentrations tested, in all assays, it was found that a Pluronic F68 coated poly (decanediol-phenylsuccinate-co-succinate) stimulated significant DNA damage driven by an oxidant mechanism, whereas the non-coated polyester analogue and the Pluronic F68 alone had no effect. The results obtained suggest that new polyesters can be synthesised with desirable properties from the materials perspective but formulation with additional excipients requires careful evaluation for drug delivery applications.

Keywords: Polyester; polycondensation; nanoparticles; polymer; cytotoxicity; hepatocyte; *in vitro*; uptake

1. Introduction

In recent years, there has been a renewed interest in polyesters as drug delivery devices due to their favorable biocompatibility and controllable biodegradation profiles [1-4]. Accordingly, polyester materials are regarded as a material of choice for biomedical applications including drug delivery [5-9], as diagnostic agents [10, 11] and for tissue engineering [12-16]. For these applications, polyesters with a range of physicochemical, biomechanical and biological properties are needed, along with appropriate biocompatibility, biodegradability and storage stability [17]. A balance of these properties can be obtained through incorporation of suitable constituent monomers into the polyester backbone.

For use as therapeutic agents, polyesters need to have strong associative interactions with active ingredients. An ability to release the drug at a suitable rate for therapy is important to reduce frequency of treatment [18]. Accordingly, there have been many variations made on the compositions and co-monomers used for polyesters, with a view to obtaining the most favorable controlled drug incorporation and release properties. More recently, there has been a strong economic and ecological drive for polymer precursors to be derived from sustainable building blocks, and for polymers to be produced with minimal use of solvents [19]. The synthesis of polyesters for drug delivery has been very thoroughly explored, with many variations around the use of poly(lactides), poly(caprolactone) and poly(carbonates) [3, 20, 21]. However, these polyesters by themselves are not easy to formulate into nanoparticles that are stable for storage in solution or for intravenous injection. Accordingly, methods are needed to enhance the colloidal properties of polyester nanoparticles, and the most simple of these, and thus the most appealing from an industrial perspective, is the surface adsorption to the nanoparticles of stabilising layers. The concept of sterically shielding hydrophobic polyester surfaces by attaching hydrophilic

polymers is well-established, with an extensive literature on adsorbed amphiphilic block co-polymers [22-27]. These types of stabilized nanoparticles have long been known to evade uptake by the mononuclear phagocyte system (MPS), [28] and so for practical drug delivery purposes there is a strong rationale to develop polyesters which are easy to synthesise from renewable resources, and which can be easily formulated into drug-loaded nanoparticles.

Here we report the synthesis of linear polyesters from the readily available monomers succinic acid, phenyl succinic acid and 1, 10-decanediol, with progressive variation with respect to the phenyl side chain content from the polyester backbone. The polymers were made using scandium (III) triflate as a catalyst under solvent-free conditions [29-33] and evaluated for drug-loading via nanoprecipitation in the presence of coumarin-6 dye. The polymer exhibiting the highest dye loading was tested for colloidal and hydrolytic stability when formulated into nanoparticles (NPs). In addition, the toxicity of polyester nanoparticles, with and without a sterically-stabilizing adsorbed Pluronic F68 block co-polymer layer. **The toxicity of these NPs was assessed *in vitro*, using the human C3A hepatocyte cell line. Hepatocytes were selected as the liver is the primary site of nanoparticle accumulation following exposure via different routes (e.g. intratracheal instillation, ingestion, intravenous injection), and existing evidence suggests that C3A cells respond similarly to primary human hepatocytes [34-37].** The internalization of coated and uncoated polymer nanoparticles by **hepatocytes** was assessed over time, and their effects on cell viability evaluated using three assays; Alamar Blue, Neutral Red, and 5-CFDA-AM [5-carboxyfluorescein diacetate, acetoxymethyl ester] CFDA-AM. The ability of nanoparticles to stimulate cytokine production (IL-8) and cause genotoxicity (DNA damage) was assessed in order to evaluate sub-lethal impacts on cell function. These data showed that while the new selected polyesters were rapidly internalized with or without the Pluronic F68 coating, there were

differences in DNA damage induced by the NP formulations which were a consequence of the combination of the coating and ‘core’ NP, and not a function of the individual components alone.

2. Experimental Section

2.1. Materials

Succinic acid (ACS reagent, $\geq 99.0\%$), Phenylsuccinic acid (98%), 1,10-Decanediol (98%), Scandium(III) triflate (99%), Coumarin-6 (98%), Pluronic F-68, deuterated chloroform (CDCl_3), 1 mM sodium pyruvate, 1% non-essential amino acids, phosphate buffer saline solution, CFDA-AM, Neutral Red, acetic acid, 95% ethanol, ammonium chloride, Triton-X100, DAPI, H_2O_2 , HBSS, low melting point agarose, agarose, lysis buffer base, dimethyl sulfoxide, HEPES, potassium chloride, Ethylenediaminetetraacetic acid [EDTA], Bovine Serum Albumin, sodium hydroxide, Tris base and GelRed were purchased from Sigma-Aldrich. All solvents were purchased from Fischer Scientific UK.

Cell culture reagents including MEM medium, foetal calf serum (FCS), 2 mM L-glutamine, 100 U/ml penicillin/streptomycin, phenol red free MEM medium, 10 x trypsin (2.5%) and 0.4% v/v Trypan Blue were purchased from Gibco, Invitrogen. The human hepatocyte cell line C3A was purchased from ATCC, Manassas, VA, USA.

2.2. Measurements

Nuclear magnetic resonance (NMR) spectra of ^1H NMR and ^{13}C NMR were recorded at 400 MHz (^1H) and 101 MHz (^{13}C) using a Bruker DPX400 Ultrashield spectrometer and deuterated chloroform (CDCl_3) as the solvent. Spectral analysis was performed using MestRENOVA 6.0.2 software copyright© 2009 Mestrelab Research S.L. All chemical shifts are

reported in ppm (δ) relative to tetramethylsilane, referenced to the chemical shifts of residual solvent resonances (CDCl_3 : δH 7.26, δC 77.16).

Fourier transform infrared (FTIR) spectroscopy was performed on solid or liquid samples using a Cary 630 FTIR spectrophotometer equipped with a single bounce diamond ATR. MicroLab software was used for data analysis.

A Polymer Laboratories GPC 50 instrument was used to determine M_n (number-average molecular weight), M_w (weight average molecular weight) and Đ (polydispersity index, M_w / M_n). The instrument was fitted with a Polymer Laboratories PLgel guard column (50×7.5 mm, $8 \mu\text{m}$) followed by a pair of PLgel Mixed-D columns (300×7.5 mm, $8 \mu\text{m}$) and a refractive index detector. The flow rate of HPLC grade CHCl_3 at 30°C was 1 mL min^{-1} . The column calibration was achieved using narrow molar mass distribution polystyrene standards. Polymer Laboratories Cirrus 3.0 software was used for data analysis.

The thermal properties of the polymers i.e. T_m (melting temperature) and T_g (glass transition temperature) were probed using a TA-Q2000 DSC (TA Instruments) under a nitrogen atmosphere. Typically, the samples (5–10 mg) were exposed to two cooling-heating cycles from -90 to 150°C at a rate of $10^\circ\text{C min}^{-1}$.

The particle sizes (z-average diameter) of nanoparticles were measured in HPLC water determined by dynamic light scattering (DLS) using a NanoZS instrument (Malvern, UK) at 25°C using 633 nm (4 mW) wavelength laser. The scattered light was detected at an angle of 173° and analysis was performed using zetasizer software version 7.03. The zeta potentials of the NPs were determined in HEPES 10 mM buffer (pH 7.4). The size and surface zeta potentials of NPs were also measured in complete MEM cell culture medium (MEM medium supplemented with

10% heat-inactivated foetal calf serum (FCS), 2 mM L-glutamine, 100 U/mL penicillin/streptomycin, 1 mM sodium pyruvate and 1% non-essential amino acids) containing 125 µg/mL of NPs.

A Tecnai G2 (FEI, Oregon, USA) microscope was utilized for transmission electron microscopy (TEM). One drop of polymer suspension in HPLC grade water (typically 25–50 µg mL⁻¹) was dropped onto a copper grid and allowed to dry in air. The sample was put on a copper grid and allowed to air dry. The imaging was performed without staining.

A Zeiss LSM880 confocal microscope was used for imaging uptake of labelled polymers and nanoparticles, and the Zeiss Zen program was used for data analysis.

2.3. Methods

2.3.1. Synthesis of Polyesters

Poly(decamethylene succinate) [PDeMS], poly(decamethylene phenylsuccinate) [PDsMPS] and their copolymers poly(decamethylene succinate-co-phenylsuccinate) [PDeMS-co-PS] were synthesized by a solvent-free melt polycondensation method (Scheme 1). The diacid and diol ratio was maintained at 1:1 in all polycondensation reactions. A scandium (III) triflate: diol ratio of $5 \cdot 10^{-4}$ (0.05 mol%) was used in all the reactions. Polymer names, abbreviations and codes along with feed compositions are given in Table 1.

Table 1. Synthesis of polyesters with different feed ratio (mol%) of succinic acid, phenylsuccinic acid and 1,10- decanediol using scandium (III) triflate as catalyst.

Polymer ^s	Code	Feed ratio (mol%)			Scandium (III) triflate (mol% of diol)
		Succinic acid	Phenylsuccinic acid	1, 10- Decanediol	

Poly(decamethylene succinate) (PDeMS)	P01	100 (0.61 g, 5.15 mmol)	0	100 #	0.05*
	P02	70 (0.42 g, 3.60 mmol)	30 (0.30 g, 1.54 mmol)	100 #	0.05*
Poly(decamethylene succinate-co-phenylsuccinate) (PDeMS-co-PS)	P03	50 (0.30 g, 2.57 mmol)	50 (0.50 g, 2.57 mmol)	100 #	0.05*
	P04	30 (0.18 g, 1.54 mmol)	70 (0.70 g, 3.60 mmol)	100 #	0.05*
Poly(decamethylene - phenylsuccinate) (PDeMPS)	P05	0	100 (1 g, 5.15 mmol)	100 #	0.05*

[§]Reaction was conducted for 21 h in bulk at 125 °C under reduced pressure. [#] For 1, 10-Decanediol 0.90 g, 5.15 mmol. * For Scandium (III) triflate 1.27 mg, 2.58 μmol

2.3.1.1. Poly(decamethylenesuccinate) [PDeMS] polymer (P01)

The polymer was synthesized by mixing succinic acid (0.61 g, 5.2 mmol, 1 eq) and 1, 10-decanediol (0.90 g, 5.2 mmol, 1 eq) in a reaction vessel at 80 °C for 30 min under stirring for melting and mixing of the monomers. Scandium (III) triflate (1.27 mg, 2.58 μmol, 5.10⁻⁴ eq) was added followed by purging of the reaction mixture with nitrogen. The reaction was continued for 3 h after increasing the temperature to 125 °C. The pressure was then reduced to 10⁻² mbar and the reaction was further continued for 18 h after which the reaction was stopped, and the mixture was allowed to cool. The resultant polymer was purified by dissolving it in a small volume of acetone and precipitated in stirred cold methanol for three times. The precipitate was filtered and dried under vacuum to obtain a solid white powder in 94% yield.

M_n : 11500 g mol⁻¹; Đ = 3.7

¹H NMR (400 MHz, CDCl₃) δ (ppm) 4.07 (CO-O-CH₂(C₈H₁₈)CH₂, bt, 4H), 2.62 (CO-CH₂-CH₂-CO, s, 4H), 1.61 (CH₂-CH₂(C₆H₁₂)CH₂-CH₂, m, 4H), 1.28 (C₂H₄(C₆H₁₂)C₂H₄, m, 12H).

^{13}C NMR (101 MHz, CDCl_3) δ (ppm) 172.5 ($\underline{\text{C}}\text{O}-\underline{\text{C}}\text{H}_2-\underline{\text{C}}\text{H}_2-\underline{\text{C}}\text{O}$), 65.0 ($\text{CO}-\text{O}-\underline{\text{C}}\text{H}_2$), 29.6 ($\text{CO}-\text{O}-\underline{\text{C}}\text{H}_2-\underline{\text{C}}\text{H}_2$), 29.4 ($\text{CO}-\underline{\text{C}}\text{H}_2-\underline{\text{C}}\text{H}_2-\text{CO}$), 29.3 ($\text{CO}-\text{O}-\underline{\text{C}}\text{H}_2\text{CH}_2-\underline{\text{C}}\text{H}_2$), 28.7 ($\text{CO}-\text{O}-\underline{\text{C}}\text{H}_2\text{CH}_2\text{CH}_2-\underline{\text{C}}\text{H}_2$), 26.0 ($\text{CO}-\text{O}-\underline{\text{C}}\text{H}_2\text{CH}_2\text{CH}_2\text{CH}_2-\underline{\text{C}}\text{H}_2$).

FTIR wavenumber (cm^{-1}): 3446 (O-H, stretching), 2920 (C-H, asymmetric stretching), 2852 (C-H, symmetric stretching), 1722 (C=O, stretching), 1421 (C-H, bending), 1153 (C-O, stretching).

2.3.1.2. Poly(decamethylene phenylsuccinate) [PDsMPS] polymer (P05)

The polymer was synthesized by the same procedure as described above except instead of succinic acid, phenyl succinic acid (1.0 g, 5.2 mmol, 1eq) was incorporated as the diacid component reacting with 1, 10- decanediol (0.90 g, 5.2 mmol, 1 eq) using scandium (III) triflate (1.3 mg, 2.6 μmol , 5.10^{-4} eq) as a catalyst. The resultant polymer was dissolved in a small volume of acetone and purified by precipitation in cold methanol three times followed by drying under vacuum to obtain a light brown viscous liquid material in 90% yield.

M_n : 11600 g mol^{-1} ; $\text{Đ} = 3.2$

^1H NMR (400 MHz, CDCl_3) δ (ppm) 7.28 ($\underline{\text{C}}_6\text{H}_5$, ring protons, m, 5H), 4.06 ($\text{CO}-\text{O}-\underline{\text{C}}\text{H}_2(\text{C}_8\text{H}_{18})\underline{\text{C}}\text{H}_2$ and $\text{CO}-\underline{\text{C}}\text{H}(\text{C}_6\text{H}_5)$, m, 5H), 3.17 ($\text{CH}(\text{C}_6\text{H}_5)-\underline{\text{C}}\text{H}_2-\text{CO}$, m, 1H), 2.68 ($\text{CH}(\text{C}_6\text{H}_5)-\underline{\text{C}}\text{H}_2-\text{CO}$, m, 1H), 1.55 ($\text{CH}_2-\underline{\text{C}}\text{H}_2(\text{C}_6\text{H}_{12})\underline{\text{C}}\text{H}_2-\text{CH}_2$, m, 4H), 1.26-1.19 ($\text{C}_2\text{H}_4(\underline{\text{C}}_6\text{H}_{12})\text{C}_2\text{H}_4$, m, 12H).

^{13}C NMR (101 MHz, CDCl_3) δ (ppm) 173.1 ($\underline{\text{C}}\text{O}-\underline{\text{C}}\text{H}(\text{C}_6\text{H}_5)-\underline{\text{C}}\text{H}_2-\text{CO}$), 171.7 ($\text{CO}-\underline{\text{C}}\text{H}(\text{C}_6\text{H}_5)-\underline{\text{C}}\text{H}_2-\underline{\text{C}}\text{O}$), 138.0, 128.9, 127.9, 127.6 (Ring carbon peaks), 65.0 ($\text{CH}_2-\text{CO}-\text{O}-\underline{\text{C}}\text{H}_2$), 47.4 ($\text{O}-\text{CO}-\underline{\text{C}}\text{H}(\text{C}_6\text{H}_5)-\underline{\text{C}}\text{H}_2-\text{CO}-\text{O}$), 37.8 ($\text{O}-\text{CO}-\underline{\text{C}}\text{H}(\text{C}_6\text{H}_5)-\underline{\text{C}}\text{H}_2-\text{CO}-\text{O}$), 29.5 ($\text{CO}-\text{O}-\underline{\text{C}}\text{H}_2-\underline{\text{C}}\text{H}_2$), 29.2 ($\text{CO}-\text{O}-\underline{\text{C}}\text{H}_2\text{CH}_2-\underline{\text{C}}\text{H}_2$), 28.6 ($\text{CO}-\text{O}-\underline{\text{C}}\text{H}_2\text{CH}_2\text{CH}_2-\underline{\text{C}}\text{H}_2$), 25.8 ($\text{CO}-\text{O}-\underline{\text{C}}\text{H}_2\text{CH}_2\text{CH}_2\text{CH}_2-\underline{\text{C}}\text{H}_2$).

FTIR wavenumber (cm^{-1}): 3452 (O-H, stretching), 2925 (C-H, asymmetric stretching), 2854 (C-H, symmetric stretching), 1729 (C=O, stretching), 1612 (aromatic C=C stretching), 1455 (C-H, bending), 1159 (C-O, stretching).

2.3.1.3. Poly(decamethylene succinate-co-phenylsuccinate) [PDeMS-co-PS] (P02, P03 and P04)

The copolymers were synthesized by reacting succinic acid, phenylsuccinic acid and 1, 10-decanediol. The feed ratio of succinic acid and phenylsuccinic acid has been given in table 3-1. The diacids : diol molar ratio was maintained at 1:1 in all polycondensation reactions.

As an example, the synthesis of polymer (P02 polymer) with 70 mol% of succinic acid and 30 mol% of phenylsuccinic acid is described here. Succinic acid (0.42 g, 3.6 mmol), phenylsuccinic acid (0.30 g, 1.5 mmol) and 1,10-decanediol (0.90 g, 5.2 mmol) were charged in a reaction vessel and heated to 80 °C for 30 min under stirring for melting and mixing of the monomers. Scandium (III) triflate (1.3 mg, 2.6 μmol) was then added and the reaction was purged with nitrogen followed by increasing the reaction temperature to 125 °C. After 3 h of reaction, the pressure was reduced to 10^{-2} mbar and the reaction was continued for 18 h after which the reaction was stopped and the mixture was allowed to cool. The resultant polymer was dissolved in a small volume of acetone and precipitated in stirred cold methanol for three times. The precipitate was filtered, washed with methanol and dried under vacuum.

The different feed ratios generated polymers with different physical properties ranging from off-white solid powders to light brown viscous liquids, with yields from 90-95%.

PDeMS-co-PS (P02)

M_n : 11500 g mol⁻¹; Đ = 2.9

¹H NMR (400 MHz, CDCl₃) δ (ppm) 7.28 (C₆H₅, ring protons, m, 2.22H), 4.07 (CO-O-CH₂(C₈H₁₈)CH₂ and CO-CH(C₆H₅), m, 4.23H), 3.19 (CH(C₆H₅)-CH₂-CO, m, 0.30H and 2.68 (CH(C₆H₅)-CH₂-CO), m, 0.30H), 2.62 (CO-CH₂-CH₂-CO), s, 2.80H), 1.61 (CH₂-CH₂(C₆H₁₂)CH₂-CH₂, m, 4.00H), 1.28 (C₂H₄(C₆H₁₂)C₂H₄, m, 12.00H).

¹³C NMR (101 MHz, CDCl₃) δ (ppm) 172.9 (CO-CH(C₆H₅)-CH₂-CO), 172.4 (CO-CH₂-CH₂-CO), 171.6 (CO-CH(C₆H₅)-CH₂-CO), 137.9, 128.7, 127.7, 127.5 (aromatic), 64.9 (CH₂-CO-O-CH₂), 47.3 (O-CO-CH(C₆H₅)-CH₂-CO-O), 37.7 (O-CO-CH(C₆H₅)-CH₂-CO-O), 29.4 (CO-O-CH₂-CH₂), 29.2 (CO-CH₂-CH₂-CO), 29.2 (CO-O-CH₂CH₂-CH₂), 28.6 (CO-O-CH₂CH₂CH₂-CH₂), 25.9 (CO-O-CH₂CH₂CH₂CH₂-CH₂).

FTIR wavenumber (cm⁻¹): 3450 (O-H, stretching), 2920 (C-H, asymmetric stretching), 2852 (C-H, symmetric stretching), 1723 (C=O, stretching), 1609 (aromatic C=C stretching), 1420 (C-H, bending), 1154 (C-O, stretching).

PDeMS-co-PS (P03)

M_n : 10100 g mol⁻¹; Đ = 3.4

¹H NMR (400 MHz, CDCl₃) δ (ppm) 7.28 (C₆H₅, ring protons, m, 2.92H), 4.07 (CO-O-CH₂(C₈H₁₈)CH₂ and CO-CH(C₆H₅), m, 4.45H), 3.19 (CH(C₆H₅)-CH₂-CO, m, 0.50H and 2.68 (CH(C₆H₅)-CH₂-CO), m, 0.50H), 2.62 (CO-CH₂-CH₂-CO), s, 2.00H), 1.61 (CH₂-CH₂(C₆H₁₂)CH₂-CH₂, m, 4.00H), 1.27 (C₂H₄(C₆H₁₂)C₂H₄, m, 12.05H).

¹³C NMR (101 MHz, CDCl₃) δ (ppm) 172.9 (CO-CH(C₆H₅)-CH₂-CO), 172.4 (CO-CH₂-CH₂-CO), 171.6 (CO-CH(C₆H₅)-CH₂-CO), 137.9, 128.7, 127.7, 127.5 (aromatic), 64.9 (CH₂-CO-O-CH₂), 47.3 (O-CO-CH(C₆H₅)-CH₂-CO-O), 37.7 (O-CO-CH(C₆H₅)-CH₂-CO-O), 29.4 (CO-O-

CH₂-CH₂), 29.2 (CO-CH₂-CH₂-CO), 29.2 (CO-O-CH₂CH₂-CH₂), 28.6 (CO-O-CH₂CH₂CH₂-CH₂), 25.9 (CO-O-CH₂CH₂CH₂CH₂-CH₂).

FTIR wavenumber (cm⁻¹): 3453 (O-H, stretching), 2925 (C-H, asymmetric stretching), 2854 (C-H, symmetric stretching), 1731 (C=O, stretching), 1605 (aromatic C=C stretching), 1423 (C-H, bending), 1159 (C-O, stretching).

PDeMS-co-PS (P04)

M_n: 11000 g mol⁻¹; Đ = 3.1

¹H NMR (400 MHz, CDCl₃) δ (ppm) 7.28 (C₆H₅, ring protons, m, 4.15H), 4.06 (CO-O-CH₂(C₈H₁₈)CH₂ and CO-CH(C₆H₅), m, 4.29H), 3.19 (CH(C₆H₅)-CH₂-CO, m, 0.70H and 2.68 (CH(C₆H₅)-CH₂-CO), m, 0.70H), 2.61 (CO-CH₂-CH₂-CO), s, 1.30H), 1.55 (CH₂-CH₂(C₆H₁₂)CH₂-CH₂, m, 4.00H), 1.26-1.20 (C₂H₄(C₆H₁₂)C₂H₄, m, 12.00H).

¹³C NMR (101 MHz, CDCl₃) δ (ppm) 172.9 (CO-CH(C₆H₅)-CH₂-CO), 172.4 (CO-CH₂-CH₂-CO), 171.6 (CO-CH(C₆H₅)-CH₂-CO), 137.9, 128.7, 127.7, 127.5 (aromatic), 64.9 (CH₂-CO-O-CH₂), 47.3 (O-CO-CH(C₆H₅)-CH₂-CO-O), 37.7 (O-CO-CH(C₆H₅)-CH₂-CO-O), 29.4 (CO-O-CH₂-CH₂), 29.2 (CO-CH₂-CH₂-CO), 29.2 (CO-O-CH₂CH₂-CH₂), 28.6 (CO-O-CH₂CH₂CH₂-CH₂), 25.8 (CO-O-CH₂CH₂CH₂CH₂-CH₂).

FTIR wavenumber (cm⁻¹): 3447 (O-H, stretching), 2925 (C-H, asymmetric stretching), 2854 (C-H, symmetric stretching), 1731 (C=O, stretching), 1608 (aromatic C=C stretching), 1428 (C-H, bending), 1159 (C-O, stretching).

2.3.2. Empty and Dye-loaded NPs formulation

NPs of synthesized polymers were prepared by a standard precipitation method with some modification [38]. Briefly, polymer (20 mg) was dissolved in 5 mL of organic solvent (acetone) to make a homogeneous organic phase. The organic phase was added drop-wise into 10 mL of HPLC grade water under stirring (1000 rpm) and stirred for 4 h at room temperature. A syringe pump was used to control the dropping rate (0.5 mL min^{-1}). The formulation was then left overnight (open vial) to ensure the complete removal of organic solvent. The NPs suspension was then passed through a membrane syringe filter (pore size: 220 nm) (Millex-LG, Millipore Co., USA) to obtain a clear formulation. The sizes and zeta potentials of the NPs formulations were measured in HPLC grade water and in 10 mM HEPES buffer (pH 7.4), respectively after appropriate dilutions ($100 \mu\text{g mL}^{-1}$). Nanoparticle formulations were stored in a refrigerator and sizes measured after 1 month using the same dilution ($100 \mu\text{g mL}^{-1}$) to determine the stability against aggregation of the particles upon storage.

Coumarin-6 dye loaded NPs were prepared by a similar method as with blank nanoparticles by adding dye in the organic phase along with polymer. Briefly, coumarin-6 (1 mg) was dissolved along with the polymer (20 mg) in acetone (5 mL) and added at a fixed rate (0.5 mL min^{-1}) to the HPLC grade water (10 mL). After 4 h of stirring, the formulations were stored overnight (open vials) to allow acetone to evaporate. The process was performed in the dark to prevent the degradation of light sensitive coumarin-6 dye. The precipitated polymer and dye was removed by filtration through a membrane filter (pore size: 220 nm). Coumarin-6 loaded NPs were passed through PD10 Desalting Column (Sephadex G-25 Medium, GE Healthcare Life Sciences) to separate the unencapsulated dye from the formulations. The purified NPs solution was used for further characterization. The Pluronic F-68 coating was achieved by the same method, i.e. where Pluronic F-68 was dissolved in an aqueous medium (0.2% w/v) to make dye loaded and empty

nanoparticles. The dye content was determined in freeze dried formulation. The freeze dried micelle was dissolved in methanol.

The drug content was determined by freeze drying an aliquot of NP suspensions, followed by dissolution in methanol and quantification by UV-visible spectrophotometry at $\lambda_{\text{max}} = 460 \text{ nm}$ (Beckman Coulter DU 800 UV spectrophotometer).

2.3.3. Degradation study of P02 NPs formulation

The degradation profile was assessed for the empty P02 NPs formulation in HPLC water (pH 7.4) and NPs formulation (in HPLC water) with *Pseudomonas cepacia* lipase (0.2 mg mL^{-1}). The NP formulations were incubated at $37 \text{ }^\circ\text{C}$. One vial from each set was collected at a predetermined time (30 days) and freeze-dried. The freeze-dried samples were then dissolved in chloroform, filtered, and analyzed by GPC to determine the change in molecular weight.

2.3.4. C3A Cell culture

C3A human hepatocellular carcinoma cells were cultured in MEM medium supplemented with 10% heat-inactivated foetal calf serum (FCS), 2 mM L-glutamine, 100 U/mL penicillin/streptomycin, 1 mM sodium pyruvate and 1% non-essential amino acids (termed MEM complete medium) and incubated at $37 \text{ }^\circ\text{C}$ and 5% CO_2 .

2.3.5. Cell Viability assessment

The cytotoxicity of the coumarin-6 labelled uncoated and Pluronic F68 coated P02 nanoparticles was determined by a fluorescence-based 3 in 1 assay [39]. This approach allows the simultaneous assessment of cell viability using the Alamar Blue (for metabolic activity), CFDA-AM (for cell membrane integrity) and Neutral Red (for lysosomal function) assays. C3A cells were seeded at a concentration of $1.56 \times 10^5 \text{ cells/cm}^2$ into a 96 well plate and incubated at $37 \text{ }^\circ\text{C}$ and 5% CO_2 for

24 h. Cells were then exposed to MEM complete medium (control), 1% triton X100 (positive control) or nanoparticles at concentrations of 4.68, 9.37, 18.75, 37.50, 75, 150 and 300 $\mu\text{g mL}^{-1}$ (100 μL /well) and incubated at 37 °C and 5% CO_2 for 24 h. Nanoparticles were prepared via dilution in complete MEM medium and briefly, gently vortexed prior to cell exposure (nanoparticles were confirmed as intact by DLS). After 24 h the supernatants were removed (and stored at -80 °C) and the cells were washed twice with phosphate buffered saline (PBS). A solution of both 1.25% v/v Alamar Blue (TREK Lab Services) and 4 μM CFDA-AM was prepared in phenol red free MEM medium and added to cells (100 μL) before incubating the cells in the dark at 37 °C and 5% CO_2 for 1 h. Fluorescence was measured on a SpectraMax M5 Microplate Reader (Molecular Devices) at an excitation/emission of 532/590 nm for Alamar Blue and an excitation/emission of 485/535 nm for CFDA-AM. Next, for the Neutral Red uptake assay, cells were washed twice using PBS, and Neutral Red (33 $\mu\text{g mL}^{-1}$) prepared in phenol red free MEM medium was added (100 μL) to cells, which were then incubated in the dark at 37 °C and 5 % CO_2 for 1 h. Following incubation, cells were washed 3 times with PBS and then acidified (1% acetic acid) 50% EtOH (in water) (100 μL). Cells were then incubated in the dark at room temperature for 20 minutes (with shaking). Fluorescence was measured in a SpectraMax M5 Microplate Reader at an excitation/emission of 532/645 nm. All experiments were repeated on different days, on at least 3 separate occasions and data reported as mean % viability (compared to the control) +/- standard error of the mean (SEM). GraphPad Prism 6 was used to analyze the statistical significance of the data.

2.3.6. Cell uptake studies

2.3.6.1. Confocal microscopy

C3A cells were seeded (6.58×10^4 cells/cm²) on 12 mm glass cover slips at 37 °C and 5% CO₂ in 24 well plates (Falcon) for 24 h. Cells were then exposed to Pluronic F68 coated and uncoated P02 nanoparticles at a sub lethal concentration (100 µg/mL) or MEM complete medium (control) for 10, 60, 240 and 1440 minutes at 37 °C and 5% CO₂. Following exposure, cells were washed twice with PBS and fixed in 3% formaldehyde (in PBS, 250 µL) for 30 minutes in the dark at room temperature. Subsequently, the plates were washed twice with PBS and incubated with 50 mM ammonium chloride (250 µL) for 10 minutes in the dark, at room temperature. Cells were then washed twice with PBS before permeabilizing with 0.1% Triton-X100 (250 µL) for 20 minutes at room temperature. The cells were washed twice with PBS and then exposed to primary antibody monoclonal anti α tubulin mouse ascites fluid clone DM1A (1:200 in PBS, Molecular Probes, 250 µL) for 1 h at room temperature. Cells were then washed twice with PBS and incubated with secondary antibody Rhodamine Red goat anti mouse IgG (1:100 in PBS, Molecular Probes, 250 µL) for 1 h at room temperature. The cells were then washed twice with PBS and incubated for 5 minutes in the dark with 1 µg mL⁻¹ DAPI (250 µL) at room temperature to stain the **nuclei**. Finally, cells were washed twice with PBS and coverslips were mounted onto glass slides with Vector shield (Vector –H1000) and edges sealed with varnish. Cells were imaged using a Zeiss LSM880 confocal microscope using the Zen program for data analyses.

2.3.6.2. Quantification of cell uptake study

C3A cells were seeded into 96 well plates at a concentration of 1.56×10^5 cells/cm² and incubated for 24 h. Cells were exposed to uncoated and coated P02 nanoparticles ($4.68\text{-}300$ µg mL⁻¹) or MEM complete medium (control) in duplicate for 10, 60, 240 and 1440 minutes at 37 °C and 5%

CO₂. Following treatment cell supernatants were removed and cells were washed twice using PBS and 0.4% v/v Trypan Blue (50 µL) was added for 10 minutes at room temperature. Cells were washed twice using PBS and then lysed with 0.2% Triton X100 in the dark at room temperature for 20 minutes. Fluorescence was measured using a SpectraMax M5 Microplate Reader at an excitation/emission of 488/550 nm. All experiments were repeated on at least 3 separate occasions. A standard curve of fluorescence for each NP (4.68-300 µg mL⁻¹) was generated to enable uptake to be quantified which was expressed as the percentage (%) of applied dose.

2.3.7. Cytokine Production: measurement of IL-8

Supernatants collected during the cytotoxicity testing were used for cytokine analysis. The level of IL-8 was quantified for selected NP concentrations (75 and 150 µg mL⁻¹) 24 h post exposure using an ELISA kit, carried out following the manufacturer's instructions (R & D systems).

2.3.8. Genotoxicity: Comet Assay

Oxidative DNA damage and DNA strand breaks were investigated using the formamidopyrimidine-DNA glycosylase (FPG) modified Comet assay. C3A cells were seeded at a concentration of 1.66x10⁵ cells/cm² into a six well plate and incubated at 37 °C for 24 h. Cells were then washed with HBSS and exposed to HBSS (control), 60 µM hydrogen peroxide (H₂O₂, positive control) or the NPs (dispersed in HBSS) at a concentration of 75 and 150 µg mL⁻¹. Cells were incubated at 37°C for 4 h and then washed with HBSS. Trypsin (0.25%, 1 mL) was used to detach the cells and complete MEM medium (3 mL) was then added to each well. The cell suspension was centrifuged at 850 g for 2 minutes and the cells then re-suspended in HBSS (1 mL). The cell suspension (20 µL) was added to low melting point agarose (240 µL). The cells (125 µL) were then pipetted onto microscope slides pre-coated with agarose. After a 10 minute period of solidification on ice, slides were placed in Coplin jars containing lysis buffer (66.75 mL lysis

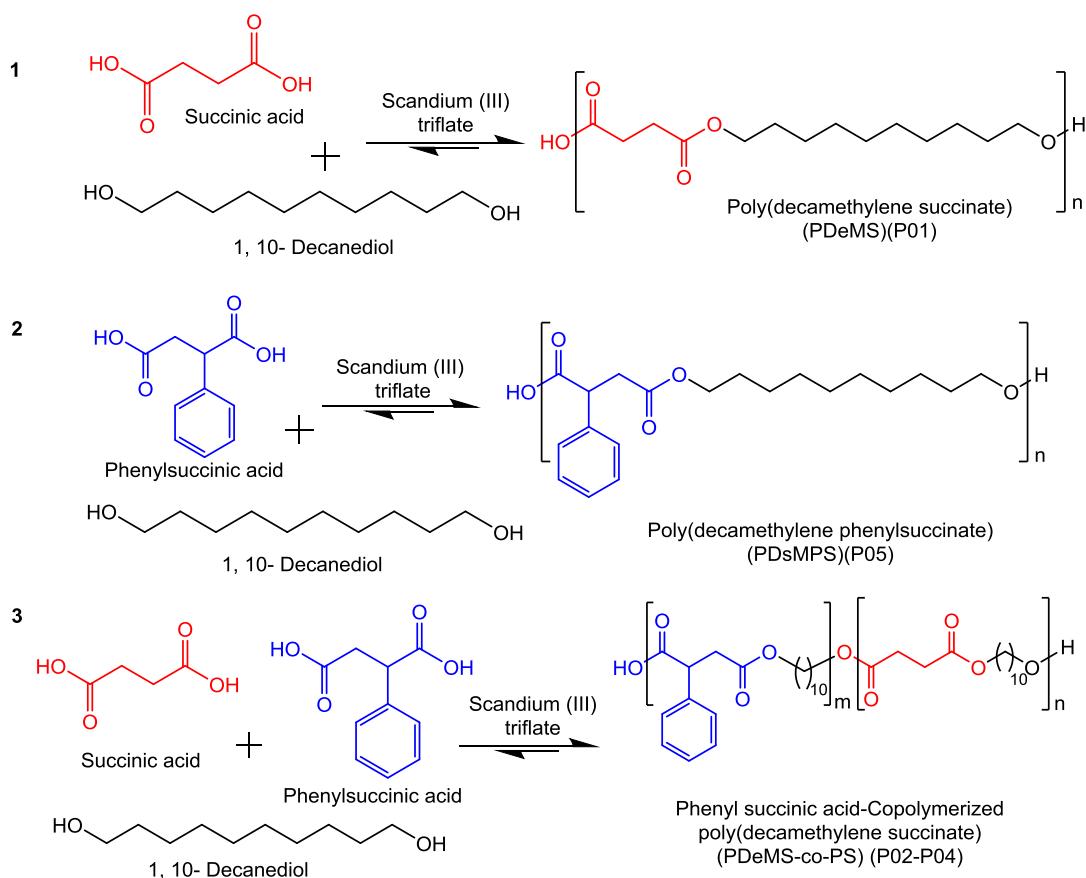
buffer base (Sigma), 7.5 mL dimethyl sulfoxide, 750 μ L Triton-X100) for 24 h at 4 °C. Slides were then washed in FPG buffer (400 mM HEPES, 1 M potassium chloride, 5 mM ethylenediaminetetraacetic acid [EDTA], 2 mg mL⁻¹ Bovine Serum Albumin, pH 8) for 15 minutes. The assay was conducted in the presence and absence of the enzyme FPG. FPG buffer or FPG enzyme in buffer (100 μ L) was added to slides, covered with a cover slip and incubated at 37 °C for 30 minutes. Slides were then transferred to a darkened electrophoresis tank cooled to 4 °C and covered with electrophoresis buffer (300 mM sodium hydroxide, 200 mM EDTA, 2 litres distilled water, pH 13). After a 20 minute period to allow for alkaline unwinding, electrophoresis was carried out for 20 minutes at 24 V and 270 mA. Slides were then removed from the tank and placed in neutralisation buffer (48.5 g Tris base, 900 mL distilled water pH 7.5) for 15 minutes at 4 °C. Slides were then dried for 15 minutes before being dipped in 100% ethanol and stained with GelRed. The tail moment (tail length x total tail intensity) was assessed using a fluorescence microscope (Zeiss AX10 with Allied Vision Technologies Stingray camera) connected to image analyzing software (Comet Assay IV: Perceptive Instruments, UK). Fifty cell measurements were recorded for each slide per experiment.

Data in Figures are means \pm standard error of the mean (SEM). Data for the two particle types were compared to the control values and each other using an ANOVA with Tukey's multiple comparison for the tail moment. All statistical tests were performed using Minitab 15. A p value <0.05 was considered a significant value. For the two particle types the experiment was repeated a minimum of three times.

3. Results

3.1. Synthesis and characterization of the polymers

The synthesis and structures of the polymers are shown in Scheme 1.



Scheme 1: Synthesis of polymers P01-P05 using polycondensation reactions.

Polyesters P01-P05 were produced from the corresponding diol and diacid monomers by solvent-free polycondensation using 0.05 % $\text{Sc}(\text{OTf})_3$ as the catalyst. The physical state of the purified final materials varied from solid to viscous liquid, depending on their co-monomer composition. The poly(decamethylene succinate) ester (P01) was a colourless solid whereas the polymers prepared with phenylsuccinic acid and decanediol were viscous light brown oils. The polymers containing both of the acid components ranged from solids to viscous oils according to phenyl content. The isolated yields of the polymers were typically 90-95%. The characterization data of the synthesis and the polymers are given in Table 2.

Table 2. Polymers (P01-P05): synthesis, composition (mol % of diacid) and molecular weight (g mol⁻¹)

Polymer Code	Feed		Product		Molecular Weight			Yield (%)
	Ratio (mol%)		Ratio (mol %)*		(g mol ⁻¹) [§]			
	SA	PSA	SA	PSA	<i>M_n</i>	<i>M_w</i>	PDI (<i>M_w/M_n</i>)	
P01	100	0	100	0	11500	42200	3.66	94
P02	70	30	70	30	11500	37600	2.87	93
P03	50	50	50	50	10100	34200	3.39	92
P04	30	70	30	70	11000	34400	3.13	91
P05	0	100	0	100	11600	37600	3.24	90

* Determined by ¹H NMR spectroscopy; [§] Determined by gel permeation chromatography (GPC) using CHCl₃ as the mobile phase. SA: Succinic acid, PSA: Phenylsuccinic acid, *M_n*: Number average molecular weight, *M_w*: Weight average molecular weight, PDI: Polydispersity Index.

The polymers showed number average molecular weights (*M_n*) ranging from 10,100-11,600 g mol⁻¹ as determined by gel permeation chromatography (GPC). The polydispersity indices were similar for all the polymers and hence the materials were considered suitable for comparative studies. The monomer composition of polyesters P01-P05 was determined by ¹H NMR spectroscopy (Figure S1, S3, S5, S7 and S9). The peak assignment was further confirmed by 2D COSY NMR (Figure S2, S4, S6, S8 and S10) and ¹³C NMR spectrum (Figure S 11).

The differential scanning calorimetry (DSC) data showed a pattern for the thermal properties of the polymers (Table 3). The melting temperature (*T_m*), crystallization temperature (*T_c*) and melting enthalpy (ΔH) were found to decrease with increasing phenyl content (Figure S12, Table 3). For P04 and P05 no *T_m* were detectable and only glass transition temperatures (*T_g*) were observed. The glass transition temperatures for all the polymers were in the -40 to -30 °C range. The P01 polymer with no phenyl side chains showed a sharp melting temperature, but no glass transition temperature

was detected. Figure S12 shows the trend in the melting temperatures (T_m), glass transitions temperatures (T_g) and crystallization temperature (T_c) of the synthesized polyesters P01-P05.

Table 3. Thermal properties and physical properties of the synthesized polyesters with different phenyl side-chain content.

Polymer Code	Product Ratio (mol%)		Thermal Property				Physical property
	SA	PSA	T_g (°C)	T_m (°C)	Melting Enthalpy (ΔH) J/g	T_c (°C)	
P01	100	0	ND	71	124	49	Crystalline
P02	70	30	-39	45	44	19	Semicrystalline
P03	50	50	-38	35	32	4	Semicrystalline
P04	30	70	-40	ND	ND	ND	Amorphous
P05	0	100	-34	ND	ND	ND	Amorphous

ND:Not detected; SA:Succinic acid; PSA:Phenylsuccinic acid. T_g : Glass transition

temperature, (T_g) (B) T_m : melting temperature; T_c : crystallization temperature

3.2. Preparation and characterization of nanoparticles

Polymers of similar molar mass but with differences in their phenyl content were investigated to determine if side-chain content and T_g/T_m variation had any effect on their ability to encapsulate model drugs. The polymers were mixed with a fluorescent dye, coumarin-6 (C log P ~ 6, as a model for highly lipophilic drugs) prior to nanoprecipitation from a common solvent (acetone) to a non-solvent (water). The characteristics of the polymers following nanoprecipitation and dye loading are given in Table 4.

Table 4 Characteristics of empty and dye loaded NPs of various polymers.

Polymer	Empty Nanoparticles [£]		Dye Loaded Nanoparticles [£]		Zeta potential (mV) (\pm SD)	Drug Content (%) \pm SD
	Average Size (nm)	PDI	Average Size (nm)	PDI		

P01	144 ± 6	0.09 ± 0.02	146 ± 9	0.10 ± 0.02	-39 ± 9	ND
P02	160 ± 7	0.03 ± 0.01	168 ± 7	0.05 ± 0.01	-40 ± 7	0.28 ± 0.01
P03	163 ± 8	0.06 ± 0.02	166 ± 5	0.07 ± 0.02	-38 ± 5	0.23 ± 0.02
P04	165 ± 6	0.10 ± 0.03	172 ± 6	0.09 ± 0.02	-39 ± 6	0.12 ± 0.01
P05	164 ± 4	0.09 ± 0.02	167 ± 7	0.08 ± 0.02	-41 ± 6	0.05 ± 0.01
P02*	185 ± 5 [‡]	0.07 ± 0.02	206 ± 6	0.08 ± 0.02	-21 ± 6 [§]	0.23 ± 0.02

*Pluronic F68-coated P02 NPs. [‡]Determined in HPLC water using Dynamic Light Scattering

(DLS) Technique. [‡]Significant difference in size from dye loaded P02* NPs ($p < 0.05$, unpaired student's t test). [§]Significant difference in zeta potential from P02 NPs ($p < 0.05$, unpaired student's t test).

At ambient temperature P01 polymer was found to be poorly soluble in the organic phase (acetone) compared to the other polymers, and needed to be dissolved at ~ 40 °C prior to nanoprecipitation. The method of nanoprecipitation was optimized for solvent to non-solvent and polymer to coumarin-6 dye ratios. A difference in the **color** intensity (yellow) was observed when the nanosuspensions were passed through a 0.22 µm filter to remove large aggregates. **No significant change in dye loading was observed when the formulation was dialyzed for 9 h using 12 kDa membranes, indicating that the dye was loaded only in the nanoparticles and was not loosely associated with the nanoparticle surfaces.** In general, the entrapped dye content was decreased as the content in phenyl side-chains in the polymer increased. No dye was detected in the NPs made from P01 polymer. The dye loading was found to be highest with PDeMS-co-PS (P02) polymer, with 30% phenylsuccinic acid in its diacid repeating units, compared to other synthesized polymers, although the overall amounts of incorporated dye were still low. The amount of incorporated coumarin-6 dye decreased as the proportion of phenyl side chains increased from 30 to 100% of total diacid content (Figure 1). Nanoparticles made from P02 polymer were also formulated for enhanced suspension stability by the adsorption of Pluronic F68, which

significantly changed the zeta potential from -40 mV to -21 mV in dilute HEPES buffer. The particle sizes of the NPs following storage for one month were statistically insignificantly different compared to those of NPs before storage ($p > 0.05$, unpaired Student's t test) indicating good colloidal stability of the formulated NPs. The dye loading was significantly decreased ($P < 0.05$, unpaired student's t test) when uncoated P02 NPs formulations were compared against the Pluronic F68 coated P02 NPs formulation, although again the overall loading was low (Figure 1).

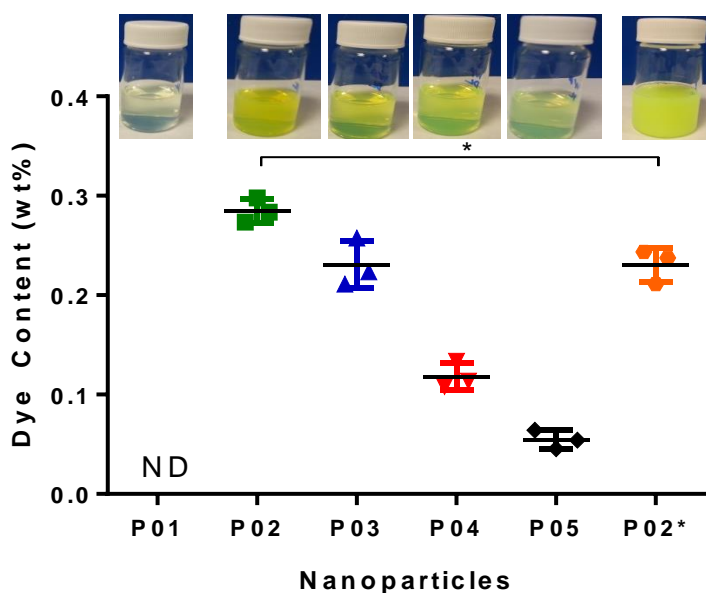


Figure 1: Coumarin 6 loading (wt% to polymer) in copolymers P01-P05. Each point represents mean dye content (wt% to polymer) \pm SD (n=3). ND: Not detected. P02*: Pluronic F68-coated P02 NPs. A significant difference in dye incorporation ($p < 0.05$, unpaired Student's t test) was observed between P02 and P02* NPs.

There was no significant difference in the sizes observed between empty and dye loaded P02 NPs. The Pluronic F68 coating significantly increased the size of the P02 NPs compared to uncoated P02 NPs and the dye loaded P02 NPs coated with Pluronic were also of significantly higher size

compared to empty Pluronic coated P02 NPs (Table 4). As expected, the Pluronic coating stabilized the P02 NPs compared to uncoated P02 NPs when diluted in PBS. Dynamic light scattering of P02 NPs in HPLC water showed essentially one population group of particles whereas two distinct populations were observed when the same uncoated P02 NPs were diluted in PBS. In contrast, Pluronic F68 coated P02 NPs retained a unimodal population distribution after dilution in both of the media (HPLC water and PBS). Additionally there was a significant difference between the zeta potential of coated (-40 ± 7) and uncoated (-21 ± 6) P02 NPs when dispersed in HEPES 10 mM buffer (pH-7.4). The TEM images of uncoated and Pluronic coated P02 NPs showed a uniform distribution of spherical nanoparticles (Figure 2).

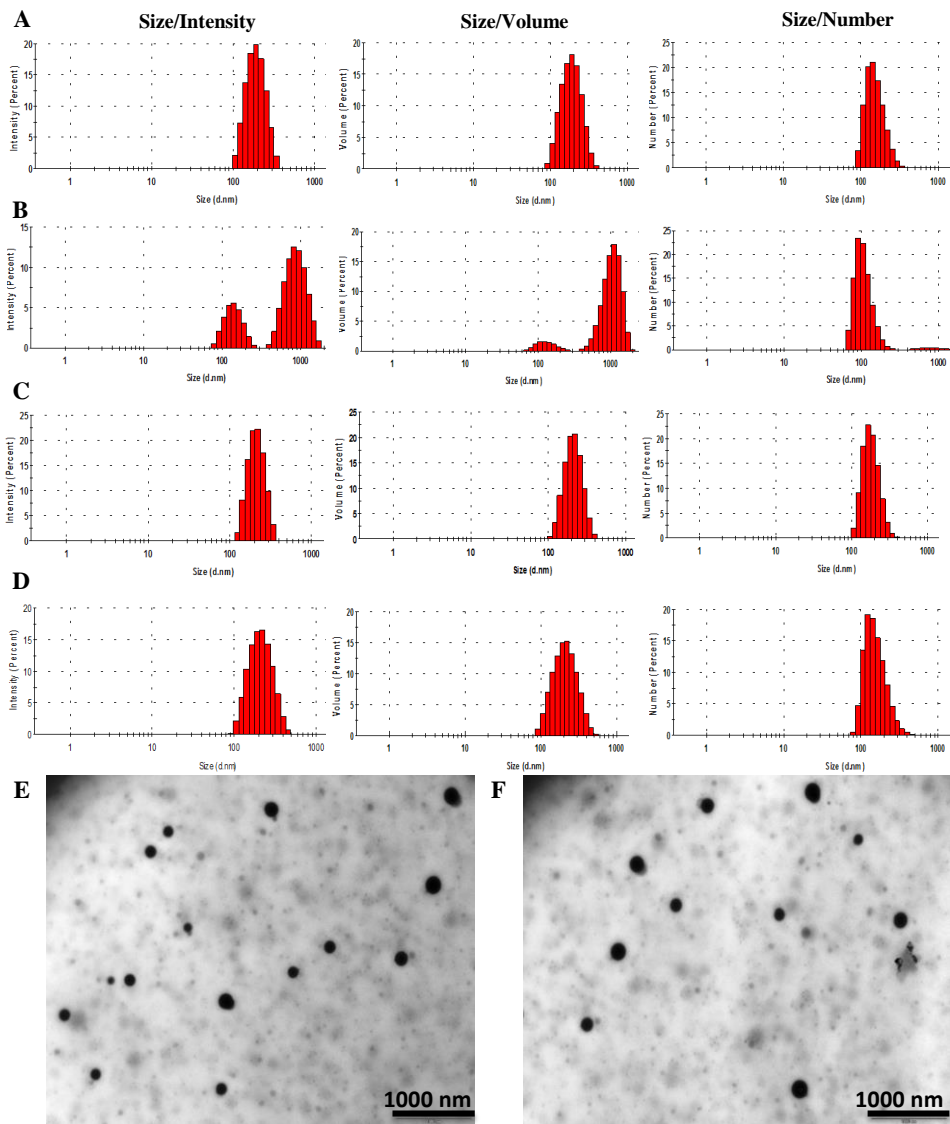


Figure 2: Size distribution of NPs as determined using DLS of suspensions ($100 \mu\text{g mL}^{-1}$) in HPLC water and PBS. (A) Uncoated P02 nanoparticles in HPLC water, (B) Uncoated P02 NPs in PBS, (C) Pluronic coated P02 NPs in HPLC water, (D) Pluronic coated P02 NPs in PBS, (E) TEM of uncoated P02 NPs, and (F) TEM of Pluronic coated P02 NPs.

As previously noted, uncoated (P02) NPs were significantly smaller ($140 \pm 1 \text{ nm}$) than coated (P02*) NPs ($146 \pm 1 \text{ nm}$) when dispersed in MEM complete medium (Table 5). The zeta potentials of P02 ($-12.67 \pm 0.37 \text{ mV}$) and P02* ($-10.68 \pm 0.75 \text{ mV}$) NPs (in MEM complete medium) were

negative. The size variations for both NPs when dispersed in complete MEM medium were low, ranging from polydispersity indices of 0.13 ± 0.01 for uncoated P02 NPs to 0.22 ± 0.01 for coated P02* NPs, therefore indicating that the NPs were stable in media as well as in HPLC water.

Table 5: Characteristics of nanoparticles in MEM complete medium.

NP	Hydrodynamic Diameter (nm) [#]	Zeta Potential (mV) [#]	Polydispersity Index (PDI) [#]
P02	140 ± 1	-12.7 ± 0.4	0.13 ± 0.01
P02*	146 ± 1 ^{\$}	-10.7 ± 0.8	0.22 ± 0.01 ^{\$}

[#] P02 and P02* NPs were dispersed in complete MEM medium (125 μ g/ml) prior to dynamic light scattering measurements. *Pluronic F68 adsorbed onto the surface of the P02 nanoparticles. ^{\$} Significant difference ($p < 0.05$) from uncoated P02 nanoparticles, Data are expressed as average \pm SEM (n = 3).

3.3. Degradation of P02 nanoparticle formulations

Polymer degradation profiles are important in polyesters designed for sustained release, as these data provide valuable information related to *in vivo* fate and long term formulation storage. Degradation of the selected P02 formulation was monitored at specific time intervals (30 days) in the presence and absence of a model hydrolytic enzyme, *Pseudomonas cepacia* lipase (0.2 mg mL⁻¹). The presence of the lipase resulted in a reduction in the polymer M_n to 53% of its original value after 3 months. Conversely, a drop of only 12% in M_n was observed in the absence of enzyme (Figure 3).

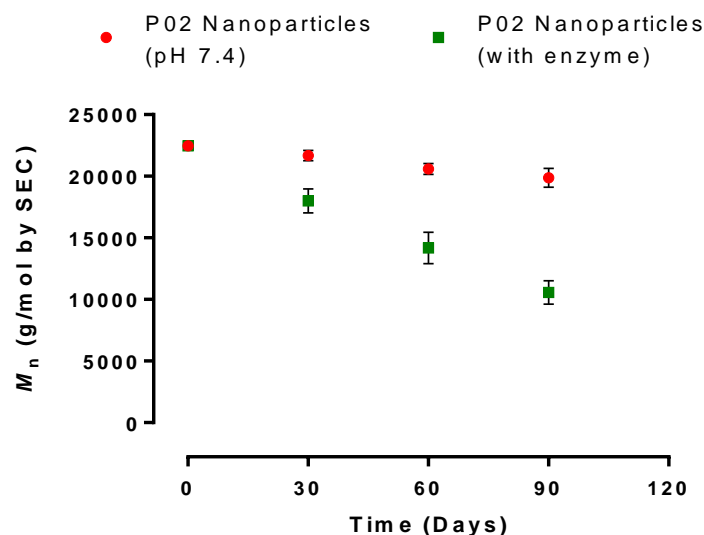


Figure 3: Loss in molar mass (M_n) of P02 NPs with time in the presence and absence of *Pseudomonas* lipase (0.2 mg mL^{-1}) at $37 \text{ }^\circ\text{C}$.

3.4. Impact of NPs on C3A cell viability

The effects following exposure of C3A hepatocytes to P02 NPs (in the presence and absence of a Pluronic F68 coating) were assessed using the Alamar Blue (AB), 5-carboxyfluorescein diacetate, acetoxymethyl ester, (CFDA-AM), and Neutral Red (NR) assays. For all assays, cell viability (as a proxy for a specific activity) was more than 80% for both coated and uncoated P02 nanoparticles 24 h post exposure, at a concentration range (4.6 to $300 \text{ } \mu\text{g mL}^{-1}$) relevant to polymeric nanomedicines administered *in vivo* (see Supplementary Information for calculations).. Although dosing at 150 and $300 \text{ } \mu\text{g mL}^{-1}$ for coated P02 (Figure 4) using the NR assay indicated a statistically significant decrease in cell viability, this was not considered to be biologically relevant as these were concentrations well above those likely to be used in a clinical setting and even at these concentrations, the overall viability decrease was no more than 20 %. Nevertheless, this decrease

might be an indicator of effects on the lysosomal function of C3A cells which could occur after accumulation of these polyester NPs.

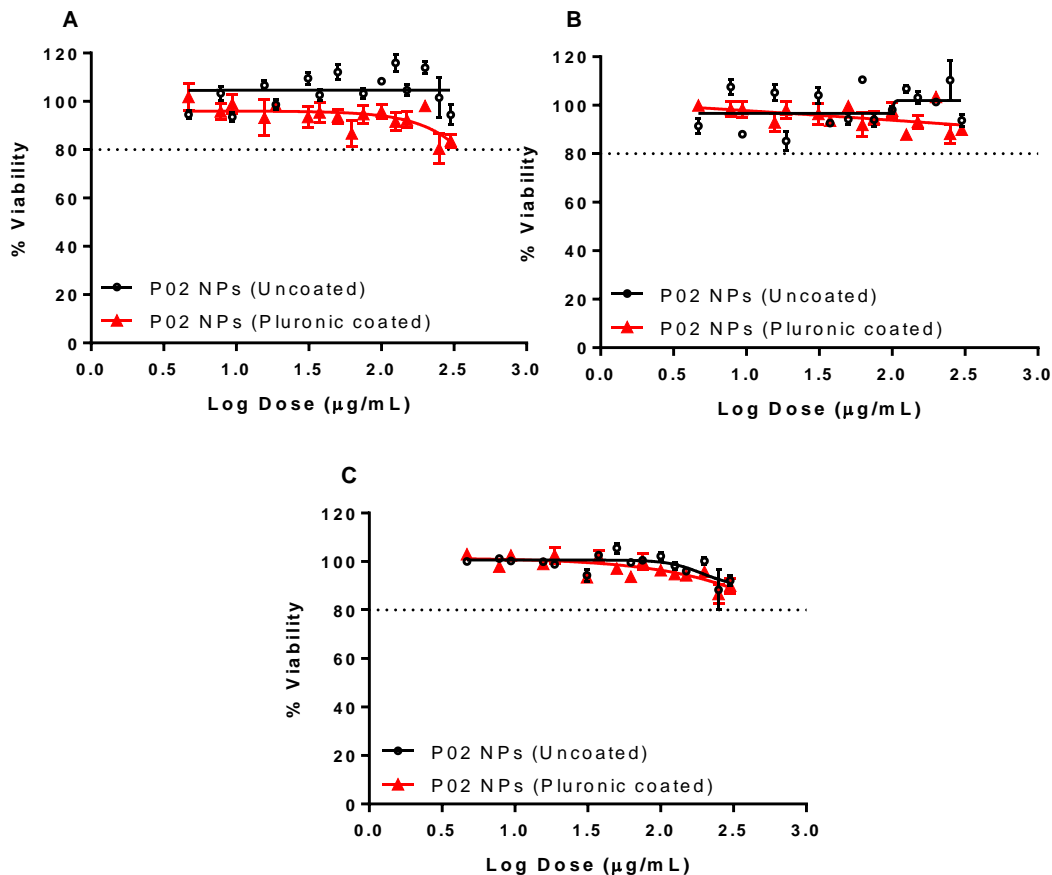


Figure 4: Viability of C3A hepatocytes following exposure to Pluronic F68 coated (red) and uncoated (black) P02 NPs. Cells were exposed to for 24 h with cell viability assessed via Alamar Blue (A), CFDA (B) and Neutral Red (C) assays. Data are expressed as the average percentage of cell viability (% of the control (MEM complete medium exposed cells) \pm SEM (n = 3 minimum)).

3.5. Cellular uptake of NPs by C3A cells

Imaging of the uptake of coated and uncoated P02 nanoparticles by C3A cells suggested that both types of the nanoparticles were readily taken up by cells within 10 min of exposure. The NPs were

present both on the surface of the cells and were internalized into the cell interior (confirmed via z stack images). The internalization of both types of P02 nanoparticles increased progressively over time from 10-1440 minutes, and in all cases NPs were predominately located within the cytoplasm of cells.

Initially (10 minutes post exposure) both types of NPs were observed to be compartmentalized inside and between the cells, although a more diffuse pattern of uptake was observed at 1440 mins (Figures 5 and 6), particularly in relation to the coated P02* NPs. In addition, some fluorescence was detected from within the nucleus after 1440 minutes but due to the resolution (approximately 200 nm) of the microscope it was not possible to distinguish individual nanoparticles. For uncoated NPs, vacuoles containing fluorescence adjacent to the nucleus could be seen from 10 min. Internalization of NPs into the cell interior were confirmed via z stacks (Figure 7).

Quantification of coated and uncoated P02 nanoparticle uptake confirmed the findings obtained from confocal microscopy. The extent of NP uptake by cells was concentration and time dependent (Figure 8). For both NP types the greatest level of uptake was observed at 1440 min. The uncoated P02 NPs showed the highest level of uptake at 3.8% of the applied dose internalized at $150 \mu\text{g mL}^{-1}$ after 1440 min treatment. The greatest level of uptake for Pluronic F68 coated P02 NPs was observed at 1440 min, with 2.7% of the applied dose internalized at a concentration of $300 \mu\text{g mL}^{-1}$.

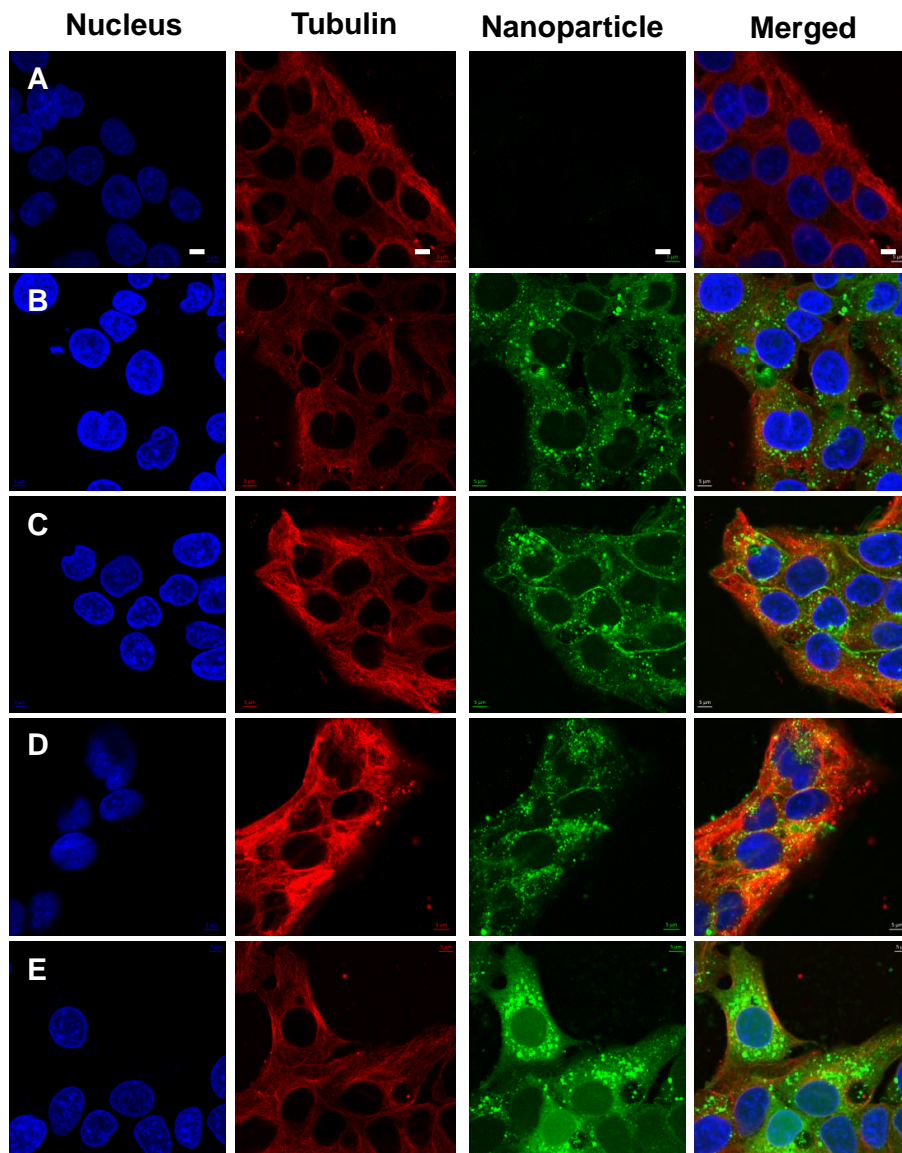


Figure 5: The time dependent uptake of coumarin-6 labelled uncoated P02 nanoparticles by C3A cells. Cells were treated with MEM complete medium (A) or NPs ($100 \mu\text{g mL}^{-1}$) for 10 (B), 60 (C), 240 or (D) 1440 minutes (E). Following exposure cells were fixed and stained for the tubulin cytoskeleton (red) and nucleus (blue). The green color represents coumarin-6 loaded NPs. Any yellow color observed indicates co-localization of tubulin and NPs. The scale bars represent $5 \mu\text{m}$.

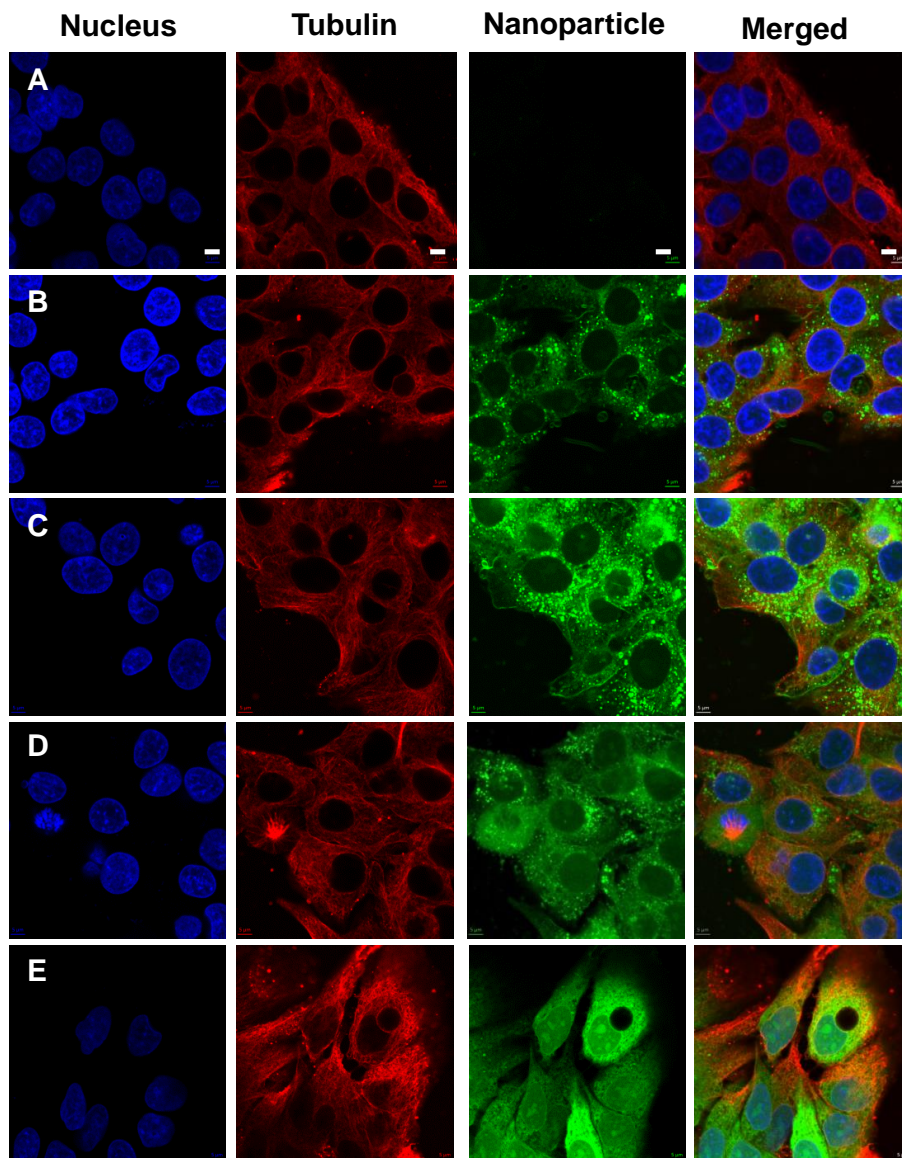
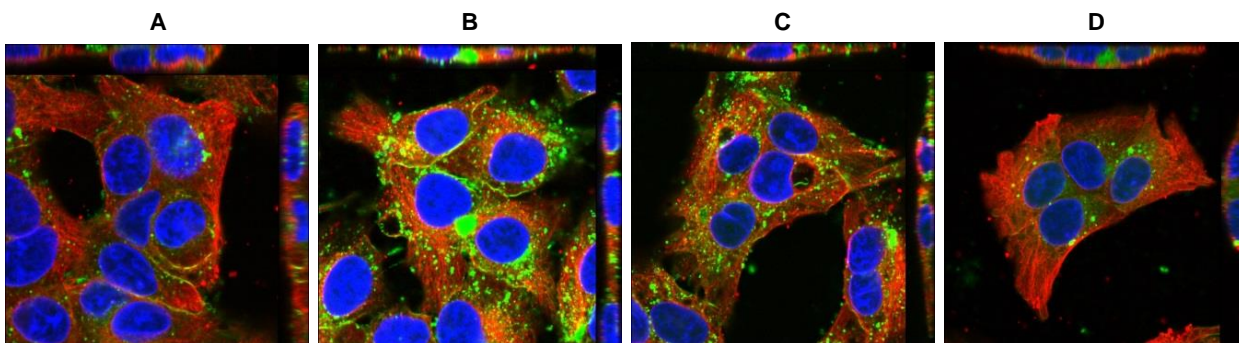


Figure 6: The time dependent uptake of coumarin-6 labelled Pluronic F68 coated P02 nanoparticles by C3A cells. Cells were treated with MEM complete medium (A) or NPs ($100 \mu\text{g mL}^{-1}$) for 10 (B), 60 (C), 240 or (D) 1440 minutes (E). Following exposure cells were fixed and stained for the tubulin cytoskeleton (red) and nucleus (blue). The green color represents coumarin-6 loaded NPs. Any yellow color observed indicates co-localization of tubulin and NPs. The scale bars represent $5 \mu\text{m}$.

P02 NPs (Uncoated)



P02 NPs (Pluronic coated)

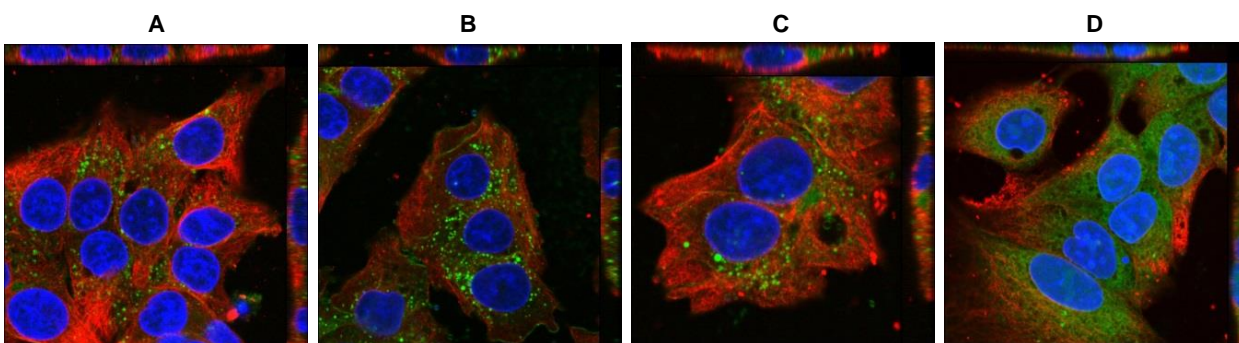


Figure 7: Internalization of uncoated P02 and Pluronic F68-coated P02 (P02*) fluorescent NPs over time by C3A cells. Images represent Z-stacks from which xy and yz micrographs were generated to confirm internalization of NPs. Cells were treated with $100 \mu\text{g mL}^{-1}$ NPs for 10 min (A), 60 min (B), 240 min (C) and 1440 min (D) and then fixed. Tubulin cytoskeleton is represented by red, the nucleus by blue and the NPs by green. Co-localization of NPs and tubulin is represented by yellow.

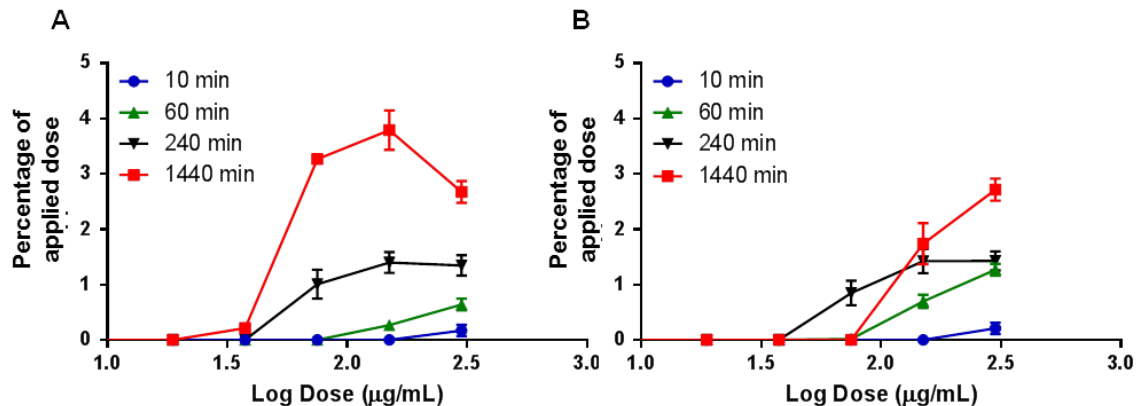


Figure 8: Quantification of the uptake of coated and uncoated P02 NPs in C3A cells over time at a range of concentrations ($4.6\text{-}300\ \mu\text{g mL}^{-1}$). Cells were treated for 10 min, 60 min, 240 min and 1440 min with uncoated P02 NPs (A) or coated P02* NPs (B). The Percent (%) applied dose was calculated from the relevant standard curves.

3.6. Cytokine Production

No change in cytokine production (IL-8) by C3A cells was detected at the NP concentrations tested 24 h post exposure, compared to the control (data not shown).

3.7. Genotoxicity

The results in Figure 9 show that at 4 h post exposure, the Pluronic F68 coated P02* NPs induced DNA damage in C3A cells at both (sub-lethal) concentrations, when tail moment was used as a measure of genotoxicity. In the absence of FPG, Pluronic coated NPs, at a concentration of $75\ \mu\text{g mL}^{-1}$, induced a significant ($p < 0.01$) 3 fold increase in DNA damage in C3A cells, when compared to the control. At a concentration of $150\ \mu\text{g mL}^{-1}$, coated NPs induced a significant ($p < 0.05$) 1.6 fold increase in DNA damage, compared to the control. In the presence of FPG, coated NPs, at a concentration of $150\ \mu\text{g mL}^{-1}$, induced a significant ($p < 0.001$) 4 fold increase in DNA damage,

compared to the control treatment (in the presence of FPG). Uncoated NPs did not induce DNA damage at the concentrations tested, in the presence or absence of FPG. The positive control H₂O₂, at a concentration 60 μM, induced significant ($p < 0.001$) DNA damage both in the presence and absence of FPG, with enhanced DNA damage observed in the presence of FPG. Pluronic F68 (alone) did not induce DNA damage (data not shown).

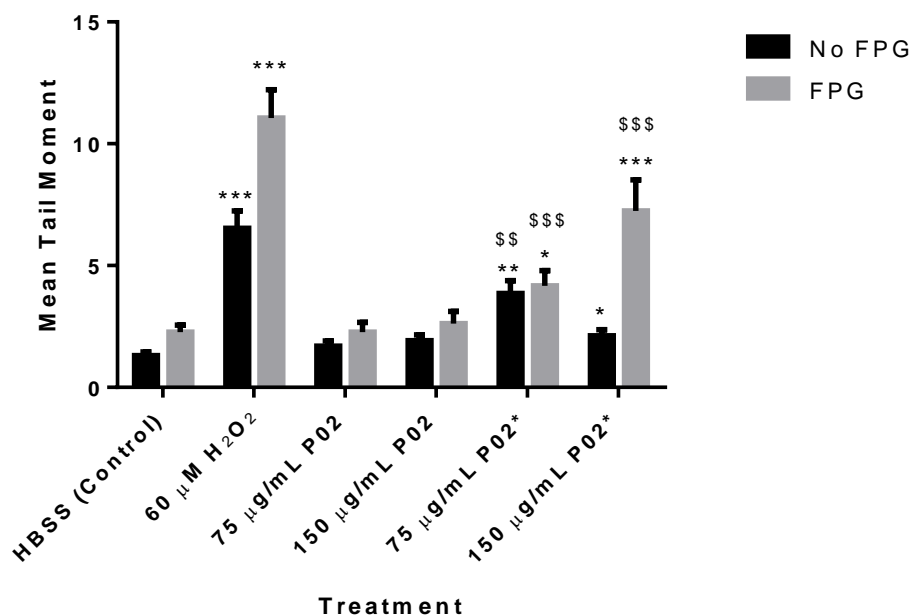


Figure 9: Genotoxicity. C3A cells were exposed to HBSS (control), 60 μM H₂O₂, P02 (uncoated) and P02* (coated) NPs (at concentrations of 75 μg mL⁻¹ and 150 μg mL⁻¹) for 4 h. DNA damage was assessed using the Comet assay in the presence and absence of FPG. Data are expressed as average tail moment ± SEM (n=3). Significance is indicated by *** = $p < 0.001$, ** = $p < 0.01$ and * = $p < 0.05$ when compared with HBSS control. \$\$\$ = $p < 0.001$ and \$\$ = $p < 0.01$ when compared to P02 (uncoated) NPs at the same concentration in the presence and absence of FPG.

4. Discussion

This study generated polyesters with varying degrees of phenyl groups in their side chains which in turn varied with respect to their crystallinity and ability to load a model drug compound. The use of scandium (III) triflate enabled the reactions to be free of organic solvent and to generate polyesters of similar molar masses repeatable over several batches of synthesis. Differences in T_g and T_m in the polymers indicated differences in chain packing of the materials: polymers with high phenyl content (P04-P05) showed only a T_g while the absence of T_m and T_c indicated that these polymers were amorphous. Since it is known that aromaticity, glassiness, and crystallinity in polymers can affect other properties such as drug loading, release and biodegradability, NPs of the polymers varying in their physical properties were prepared in the presence of a dye molecule (coumarin-6). The highest loading of coumarin-6 was observed for the P02 polymeric NPs. This was not expected from first principles as the ring systems of the dye were expected to interact more favorably with polymers containing high phenyl content through mutual π - π interactions. In addition, the polymers with higher phenyl content were amorphous hence were expected to encapsulate more dye due to the higher free volumes in the amorphous core regions. These initially contradictory results can be explained by considering three factors important during nanoprecipitation; (1) polymer-polymer interaction (2) dye-dye interaction (3) dye-polymer interaction. For a higher loading, a favorable dye-polymer interaction is important to maintain a close proximity of dye and polymer during the late stages of nanoprecipitation. However, a higher polymer-polymer interaction and dye-dye interaction can cause a reduction in the dye loading during nanoprecipitation. For the P01 polymer, which contained no phenyl succinate residues, it is likely that a high polymer-polymer and dye-dye interaction caused the molecules to precipitate resulting in a low yield of well-defined NPs and with no detectable dye content. As the phenyl content was increased for the P02 polymer, a more favorable interaction between dye and polymer

may have resulted hence the higher dye loading. However, upon further increase of phenyl content in the polymer (P03, P04 and P05), the higher π - π interactions between polymer molecules, rather than dye-polymer molecules resulted in lower loading capabilities. Since the P02 polymer (70:30 succinic acid and phenyl succinic acid) exhibited the highest dye loading capability when formulated into NPs, subsequent assessment of the degradability of the polymers and its effects on hepatic cells were prioritised. Molar mass profiles over time revealed that P02 polymer NPs were degradable, although the low degradation rate of the polymer at pH 7.4 indicated that the polymer was quite resistant to primary hydrolytic cleavage. The presence of esterolytic enzymes increased the degradation rate suggesting that the polymer should be degraded in the body more rapidly if in contact with endogenous esterases.

Prior to cytocompatibility experiments, potential factors affecting cell association uptake and uptake of the polymeric nanoparticles were evaluated. The hydrodynamic diameters of P02 (uncoated) NPs were less than those of P02* (coated) NPs, as expected due to the absorbed Pluronic coating on P02* NPs but the differences were less than 10% so were unlikely to impact on endocytic uptake mechanisms.[40] There is evidence that particle charge influences particle-cell interactions and uptake, and the charge of NPs can also reflect dispersion stability and the potential for agglomeration. As a consequence zeta potential is often used as an indicator of charge when characterizing NP properties.[41] The zeta potentials of both P02 and P02* NPs were negative, ranging from -10.7 to -12.7 mV, and in biologically relevant media the differences in zeta potential between the coated and uncoated NPs were not statistically significant, suggesting that NP charge alone was unlikely to influence particle-cell interactions.

A 3 in 1 assay (Alamar Blue, CFDA-AM and Neutral Red) was used to assess viability of cells exposed to the polymer NPs. Furthermore, using 3 different assays which assess different cell

responses as indicators of cytotoxicity can provide information on the mechanism of NP toxicity. All three assays indicated that the coated and uncoated P02 NPs exhibited low acute toxicity in the experimental conditions tested. A greater sensitivity was observed with the Neutral Red assay showing statistically significant effects on normal lysosome function at high concentrations of Pluronic F68 coated P02 NPs, although the small changes in cell viability observed were not considered to be of potential biological significance.

Assessment of cytotoxicity at 24 h allows for comparison of results obtained in this study to those obtained in prior literature as the majority of nanotoxicology studies evaluate cytotoxicity 24 h post exposure using the C3A cell line and other cell types (e.g. immune cells, epithelial cells).[42, 43] A limitation of *in vitro* studies is that it is more challenging to assess chronic toxicity. In future studies the development of *in vitro* assays which enable toxicity to be assessed after repeated exposures or longer exposure periods would allow for the assessment of recovery or increased cytotoxicity over time.

In order to evaluate the toxic potency of NPs, the lethal concentration (LC50) can be calculated, which identifies the concentration of NPs required to kill 50% of cells. No LC50 values could be calculated for the NPs tested in this study, despite concentrations up to 300 $\mu\text{g mL}^{-1}$ being tested. Previous studies which have investigated the response of C3A cells to engineered NPs (e.g. silver, zinc oxide) at a similar concentration range tested in this study, have calculated LC50 values of approx. 2 $\mu\text{g mL}^{-1}$ [44], demonstrating the relatively low toxicity of the polymeric NPs tested in this study.

Toxicity testing is performed in different phases. By screening the toxicity of the polymeric NPs *in vitro* in the first instance, a rapid assessment of the toxicity of NPs of varied physico-chemical

properties is possible. Performing *in vitro* studies also allowed the mechanism of toxicity to be probed in a cost and time efficient manner, and ensured that the study was aligned with the 3Rs principles (reduction, refinement and replacement of animal testing). Although cell lines can lose functions present in primary cells and therefore have been criticized for their lack of relevancy, previous studies have demonstrated that the C3A cell line is able to replicate the response of human and rat primary cells to many different types of NPs [44]. This is particularly important as it is well established that cells vary widely in their sensitivity when exposed to a range of nanomaterials [45].

NPs are known to elicit toxicity via mechanisms involving stimulation of inflammation and oxidative stress [46], which are driven by their physico-chemical characteristics (e.g. composition, size, charge). The stimulation of inflammatory and oxidant driven responses can induce a number of downstream consequences such as genotoxicity or cell death. Cytokine production was used as an indicator of the pro-inflammatory effects of the NPs in this study. No IL-8 production was stimulated by NPs following exposure of C3A cells. NPs such as silver and zinc oxide have previously been observed to stimulate IL-8 production [44], oxidative stress [47] and genotoxicity [47] in C3A cells. Additionally, *in vivo* studies in mice using cationic NPs for DNA delivery have shown increased levels of chemokine KC, the homolog of human IL-8.[48] Accordingly assessment of NP mediated IL-8 production from hepatocytes was prioritised in this study. No changes in IL-8 production were observed following exposure of cells to P02 and P02* NPs, and while we cannot rule out production of other cytokines (e.g. TNF- α , IL-6) in response to stimulation by NPs in these C3A cells, our primary screen based on IL-8 suggested no exceptional pro-inflammatory activation. It is also possible that any cytokine proteins produced by cells may

also have adsorbed to the NP surfaces, preventing their detection [49], although we did not specifically measure for adsorbed proteins.

Pluronic F68-coated NPs were observed to stimulate DNA damage in C3A cells, whilst uncoated NPs did not induce a response. DNA damage induced by Pluronic coated NPs was enhanced in the presence of FPG which suggests that the damage is mediated by an oxidant mechanism. The NPs themselves may have had intrinsic oxidative activity, as well as the ability to induce production of intracellular reactive oxygen species (ROS) when interacting with the cells to result in an imbalance between oxidants and antioxidants within the cell.[50] Data obtained suggested that the Pluronic F68 coating enhanced the genotoxicity of the NPs in this study. It has been previously shown that certain Pluronic co-polymers can elicit transcriptional activation in cell lines under certain conditions, and effects on complement activation have been known for these polymers for many years [51, 52]. However, it is unlikely that the genotoxicity observed here derived from the leaching of the amphiphilic co-polymer from the NP surfaces, as when Pluronic F68 alone was administered to cells, at a concentration equivalent to that contained in the NPs, no genotoxicity was observed. Nevertheless, since the properties of different Pluronics change with concentration and aggregation status [53] a possible effect on key cellular components of Pluronics associated at block co-polymer surfaces cannot be ruled out. Work by Kabanov *et al* demonstrated that Pluronic P85 co-polymers were able to cause energy-depleting effects in multi-drug resistant (MDR) cells, [54] where it was suggested that depletion occurred partially by membrane permeabilisation and possible release of reactive oxygen species (ROS). In prior studies of mitochondrial membrane disruption [55], Pluronic P85 was shown to be less potent than Pluronic F68 but more active than a higher molar mass Pluronic, L121. These previous data had indicated a 'hotspot' of membrane-disruption for the Pluronic co-polymers with central hydrophobic

poly(propylene oxide) block lengths of ~2000 Da, similar to that in Pluronic F68. Specific effects of the F68 coating may thus have accounted for the observed increase in genotoxicity, and it should be noted that Pluronic F68 has been shown to increase the production of interferon γ in Chinese Hamster Ovary cells, [56] albeit at much higher concentrations than in our assays, through a mechanism that likely involved partial or temporary membrane modification.

Evaluation of the uptake and intracellular fate of nanoparticles intended for medical use is important as carrier materials are often required to enter the cell in order to deliver a therapeutic or identify a disease phenotype [57]. Previous studies have indicated that uptake efficiency and subcellular localisation can influence material cytotoxicity [58]. Therefore, it is important to elucidate the uptake pattern of the polyester NPs, particularly in hepatic cell lines, as it is well established that the liver is a site of accumulation for many nanoparticles following exposure via various routes (e.g. intravenous injection, ingestion, inhalation/intratracheal instillation) [34, 35, 37]. The uptake of coated and uncoated P02 NPs in C3A cells suggested that the NPs were taken up by the cells in a time and concentration dependent manner. Previous studies have indicated that the uptake of polymer NPs by cells increased with time in other cell lines (e.g. macrophages), although these studies did not look at the impact of NP concentration on uptake and assessed uptake over a shorter time frame [59, 60]. Different cell types vary with respect to their efficiency at internalising NPs. Existing studies have investigated the uptake of NPs by macrophages *in vivo* and *in vitro*, due to their prominent role in particle clearance from the body (e.g. lungs, liver). The predominant mechanism of particle uptake by hepatocytes and thus the most likely route of uptake in this study is endocytosis, which has a lower efficiency than phagocytosis. Interestingly, similar overall levels of uptake compared to those of P02 and P02* in C3A cells have been noted for carboxymethyl chitosan NPs in the L02 hepatocyte cell line.[61] In this study the polyester NPs

were primarily compartmentalized within and between C3A cells as early as 10 minutes post exposure. At the later time point of 1440 minutes the polyester NPs were observed throughout the cytoplasm of the C3A cells. The subcellular fate of internalized NPs was not investigated in this study, however the pattern of uptake observed suggests that these particular NPs were initially located within the cell organelles such as endosomes or lysosomes. P02 NPs were observed to accumulate in lysosomes of the J774 macrophage cell line 1 h post exposure (data not shown) and polystyrene NPs and quantum dots have also been observed to accumulate in lysosomes and mitochondria of macrophages *in vitro* [62]. Current studies are investigating the subcellular localization to better understand the fate of internalized polyesters from these formulations.

NPs were also seen to accumulate between cells, which may be representative of accumulation in bile canaliculi. These structures are responsible for the formation and secretion of bile by hepatocytes and could be indicative of NP removal from the cells. Interestingly, the elimination of polystyrene NPs (20 nm) in bile has been observed previously *in vitro* and *in vivo* [60].

The co-localization of NPs with tubulin was also observed in this study, particularly within the perinuclear region of the cell. Research has shown that tubulin may be involved with the directional transport of NPs within the cell and this transport can be targeted towards the nucleus [63]. NPs in vacuoles in close proximity to the nucleus could also suggest targeted delivery to the nucleus, although the size of these particular NPs would likely prohibit them crossing an undamaged nuclear membrane. At 24 h post exposure, coated NPs appeared to become diffuse throughout the cell, whilst the majority of uncoated NPs remained compartmentalized, suggesting that the Pluronic coating may have had an impact on the intracellular fate of NPs. NPs may thus have been partially degraded within certain cell organelles (e.g. lysosomes) via hydrolytic enzymes known to degrade polyesters [64], and thus any dye associated near the NP surfaces may have been

released into the cytoplasm. It is also possible that the P02 NPs escaped the organelles to distribute throughout the cytoplasm. An increase in the number and size of vacuoles within cells treated with Pluronic coated (P02*) NPs was also apparent which may indicate damage to the cells had occurred over time.

5. Conclusion

In this study, the synthesis of a new series of polyesters by melt polycondensation under solvent-free conditions has been described and the effects of co-monomer content on polymer properties (e.g. crystallinity) and nanoparticle properties (e.g. size, dye loading) relevant to controlled release applications have been evaluated. The study suggested that side chain phenyl content changed the loading capability of NPs for a model dye, but the overall level of incorporation remained very low. The study provided information about the stability, and degradability of a selected P02 polymer when formulated into Pluronic coated and uncoated nanoparticles. The cellular studies revealed that P02 NPs displayed low cell toxicity and were effectively taken up by the cells. However, the Pluronic coating appeared to enhance some aspects relating to the toxicity of the NPs, and this information should be used to inform the design of formulated NPs in the future.

Conflict of interest statement

The authors declare that there are no conflicts of interest.

Acknowledgments

We thank the Indian Government for a PhD Scholarship to DK. We thank Heriot Watt University for a James Watt PhD scholarship to LGP. We also thank the Engineering and Physical Sciences

Research Council (EPSRC) for financial support (Leadership Fellowship to CA, Grants EP/H005625/1 and EP/J021180/1) and Christy Grainger-Boulty and Paul Cooling for technical assistance. We would like to thank Dr Lesley Young (Edinburgh Napier University) for her assistance in confocal microscopy.

Data access statement

All raw data created during this research are openly available from the corresponding author (Cameron.alexander@nottingham.ac.uk) and at the University of Nottingham Research Data Management Repository (<https://rdmc.nottingham.ac.uk/>) and all analysed data supporting this study are provided as supplementary information accompanying this paper.

References

- [1] A.C. Albertsson, I.K. Varma, Aliphatic polyesters: Synthesis, properties and applications, *Degradable Aliphatic Polyesters*, 157 (2002) 1-40.
- [2] U. Edlund, A.C. Albertsson, Polyesters based on diacid monomers, *Advanced Drug Delivery Reviews*, 55 (2003) 585-609.
- [3] H. Seyednejad, A.H. Ghassemi, C.F. van Nostrum, T. Vermonden, W.E. Hennink, Functional aliphatic polyesters for biomedical and pharmaceutical applications, *Journal of Controlled Release*, 152 (2011) 168-176.
- [4] T. Ishigaki, W. Sugano, M. Ike, Y. Kawagoshi, I. Fukunaga, M. Fujita, Abundance of polymers degrading microorganisms in a sea-based solid waste disposal site, *Journal of Basic Microbiology*, 40 (2000) 177-186.
- [5] H.M. Aliabadi, A. Mahmud, A.D. Sharifabadi, A. Lavasanifar, Micelles of methoxy poly(ethylene oxide)-b-poly(epsilon-caprolactone) as vehicles for the solubilization and controlled delivery of Cyclosporine A, *Journal of Controlled Release*, 104 (2005) 301-311.
- [6] M.L. Adams, A. Lavasanifar, G.S. Kwon, Amphiphilic block copolymers for drug delivery, *Journal of Pharmaceutical Sciences*, 92 (2003) 1343-1355.
- [7] S. Elhasi, R. Astaneh, A. Lavasanifar, Solubilization of an amphiphilic drug by poly(ethylene oxide)-block-poly(ester) micelles, *European Journal of Pharmaceutics and Biopharmaceutics*, 65 (2007) 406-413.
- [8] Z. Ma, A. Haddadi, O. Molavi, A. Lavasanifar, R. Lai, J. Samuel, Micelles of poly(ethylene oxide)-b-poly(epsilon-caprolactone) as vehicles for the solubilization, stabilization, and controlled delivery of curcumin, *Journal of Biomedical Materials Research Part A*, 86A (2008) 300-310.
- [9] L.A. Dailey, M. Wittmar, T. Kissel, The role of branched polyesters and their modifications in the development of modern drug delivery vehicles, *Journal Of Controlled Release*, 101 (2005) 137-149.
- [10] P. Sharma, S. Brown, G. Walter, S. Santra, B. Moudgil, Nanoparticles for bioimaging, *Advances in Colloid and Interface Science*, 123 (2006) 471-485.

- [11] J.R. McCarthy, R. Weissleder, Multifunctional magnetic nanoparticles for targeted imaging and therapy, *Advanced Drug Delivery Reviews*, 60 (2008) 1241-1251.
- [12] M.A. Woodruff, D.W. Hutmacher, The return of a forgotten polymer-Polycaprolactone in the 21st century, *Progress in Polymer Science*, 35 (2010) 1217-1256.
- [13] Y.D. Wang, G.A. Ameer, B.J. Sheppard, R. Langer, A tough biodegradable elastomer, *Nature Biotechnology*, 20 (2002) 602-606.
- [14] H. Seyednejad, D. Gawlitta, W.J.A. Dhert, C.F. van Nostrum, T. Vermonden, W.E. Hennink, Preparation and characterization of a three-dimensional printed scaffold based on a functionalized polyester for bone tissue engineering applications, *Acta Biomaterialia*, 7 (2011) 1999-2006.
- [15] R.N. Shirazi, W. Ronan, Y. Rochev, P. McHugh, Modelling the degradation and elastic properties of poly(lactic-co-glycolic acid) films and regular open-cell tissue engineering scaffolds, *Journal of the Mechanical Behavior of Biomedical Materials*, 54 (2016) 48-59.
- [16] H. Kenar, G.T. Köse, V. Hasirci, Tissue engineering of bone on micropatterned biodegradable polyester films, *Biomaterials*, 27 (2006) 885-895.
- [17] B.D. Utery, L.S. Nair, C.T. Laurencin, Biomedical Applications of Biodegradable Polymers, *Journal of Polymer Science Part B-Polymer Physics*, 49 (2011) 832-864.
- [18] S. Mura, P. Couvreur, Nanotheranostics for personalized medicine, *Advanced Drug Delivery Reviews*, 64 (2012) 1394-1416.
- [19] J. Thevenot, H. de Oliveira, O. Sandre, L. Pourtau, E. Andres, S. Miraux, E. Thiaudiere, E. Berra, S. Lecommandoux, Multifunctional polymersomes for cancer theranostics, *Journal of Controlled Release*, 172 (2013) E44-E45.
- [20] C. Jérôme, P. Lecomte, Recent advances in the synthesis of aliphatic polyesters by ring-opening polymerization, *Advanced Drug Delivery Reviews*, 60 (2008) 1056-1076.
- [21] H. Tian, Z. Tang, X. Zhuang, X. Chen, X. Jing, Biodegradable synthetic polymers: Preparation, functionalization and biomedical application, *Progress in Polymer Science*, 37 (2012) 237-280.
- [22] A. Pitto-Barry, N.P.E. Barry, Pluronic (R) block-copolymers in medicine: from chemical and biological versatility to rationalisation and clinical advances, *Polymer Chemistry*, 5 (2014) 3291-3297.
- [23] L. Li, L. Mu, V. Torchilin, Mixed micelles made of pluronic and PEG-PE for solubilization of poorly soluble anticancer drug paclitaxel, *J. Drug Deliv. Sci. Technol.*, 17 (2007) 389-392.
- [24] S.M. Moghimi, A.C. Hunter, Poloxamers and Poloxamines in Nanoparticle Engineering and Experimental Medicine, *Trends in Biotechnology*, 18 (2000) 412-420.
- [25] R.J. Green, S. Tasker, J. Davies, M.C. Davies, C.J. Roberts, S.J.B. Tandler, Adsorption of PEO-PPO-PEO triblock copolymers at the solid/liquid interface: A surface plasmon resonance study, *Langmuir*, 13 (1997) 6510-6515.
- [26] J.C. Neal, S. Stolnik, M.C. Garnett, S.S. Davis, L. Illum, Modification of the copolymers poloxamer 407 and poloxamine 908 can affect the physical and biological properties of surface modified nanospheres, *Pharmaceutical Research*, 15 (1998) 318-324.
- [27] S. Stolnik, L. Illum, S.S. Davis, Long Circulating Microparticulate Drug Carriers, *Advanced Drug Delivery Reviews*, 16 (1995) 195-214.
- [28] L. Illum, S.S. Davis, R.H. Müller, E. Mak, P. West, The organ distribution and circulation time of intravenously injected colloidal carriers sterically stabilized with a blockcopolymer - poloxamine 908, *Life Sciences*, 40 (1987) 367-374.
- [29] C. Hahn, S. Wesselbaum, H. Keul, M. Moller, OH-functional polyesters based on malic acid: Influence of the OH-groups onto the thermal properties, *European Polymer Journal*, 49 (2013) 217-227.
- [30] A. Takasu, Y. Iio, Y. Oishi, Y. Narukawa, T. Hirabayashi, Environmentally benign polyester synthesis by room temperature direct polycondensation of dicarboxylic acid and diol, *Macromolecules*, 38 (2005) 1048-1050.
- [31] A. Takasu, Y. Shibata, Y. Narukawa, T. Hirabayashi, Chemoselective dehydration polycondensations of dicarboxylic acids and diols having pendant hydroxyl groups using the room temperature polycondensation technique, *Macromolecules*, 40 (2007) 151-153.

- [32] A. Takasu, Y. Oishi, Y. Iio, Y. Inai, T. Hirabayashi, Synthesis of aliphatic polyesters by direct polyesterification of dicarboxylic acids with diols under mild conditions catalyzed by reusable rare-earth triflate, *Macromolecules*, 36 (2003) 1772-1774.
- [33] A. Takasu, H. Tsuruta, Y. Narukawa, Y. Shibata, M. Oshimura, T. Hirabayashi, Dual catalytic system for combination of chain and step polymerizations: Ring-opening polymerization of epsilon-caprolactone and successive dehydration polycondensation with dicarboxylic acid using the same catalyst, *Macromolecules*, 41 (2008) 4688-4693.
- [34] C. Schleh, M. Semmler-Behnke, J. Lipka, A. Wenk, S. Hirn, M. Schaeffler, G. Schmid, U. Simon, W.G. Kreyling, Size and surface charge of gold nanoparticles determine absorption across intestinal barriers and accumulation in secondary target organs after oral administration, *Nanotoxicology*, 6 (2012) 36-46.
- [35] S. Hirn, M. Semmler-Behnke, C. Schleh, A. Wenk, J. Lipka, M. Schaeffler, S. Takenaka, W. Moeller, G. Schmid, U. Simon, W.G. Kreyling, Particle size-dependent and surface charge-dependent biodistribution of gold nanoparticles after intravenous administration, *European Journal of Pharmaceutics and Biopharmaceutics*, 77 (2011) 407-416.
- [36] E. Sadauskas, N.R. Jacobsen, G. Danscher, M. Stoltenberg, U. Vogel, A. Larsen, W. Kreyling, H. Wallin, Biodistribution of gold nanoparticles in mouse lung following intratracheal instillation, *Chemistry Central Journal*, 3 (2009).
- [37] M. Semmler-Behnke, W.G. Kreyling, J. Lipka, S. Fertsch, A. Wenk, S. Takenaka, G. Schmid, W. Brandau, Biodistribution of 1.4-and 18-nm Gold Particles in Rats, *Small*, 4 (2008) 2108-2111.
- [38] U. Bilati, E. Allemann, E. Doelker, Development of a nanoprecipitation method intended for the entrapment of hydrophilic drugs into nanoparticles, *European Journal of Pharmaceutical Sciences*, 24 (2005) 67-75.
- [39] M. Connolly, M.-L. Fernandez-Cruz, A. Quesada-Garcia, L. Alte, H. Segner, J.M. Navas, Comparative Cytotoxicity Study of Silver Nanoparticles (AgNPs) in a Variety of Rainbow Trout Cell Lines (RTL-W1, RTH-149, RTG-2) and Primary Hepatocytes, *International Journal of Environmental Research and Public Health*, 12 (2015) 5386-5405.
- [40] C. He, Y. Hu, L. Yin, C. Tang, C. Yin, Effects of particle size and surface charge on cellular uptake and biodistribution of polymeric nanoparticles, *Biomaterials*, 31 (2010) 3657-3666.
- [41] A.M. Abdelmonem, B. Pelaz, K. Kantner, N.C. Bigall, P. del Pino, W.J. Parak, Charge and agglomeration dependent in vitro uptake and cytotoxicity of zinc oxide nanoparticles, *Journal of Inorganic Biochemistry*, 153 (2015) 334-338.
- [42] D.M. Brown, H. Johnston, E. Gubbins, V. Stone, Cytotoxicity and Cytokine Release in Rat Hepatocytes, C3A Cells and Macrophages Exposed to Gold Nanoparticles-Effect of Biological Dispersion Media or Corona, *Journal of Biomedical Nanotechnology*, 10 (2014) 3416-3429.
- [43] A. Kermanizadeh, G. Pojana, B.K. Gaiser, R. Birkedal, D. Bilanicova, H. Wallin, K.A. Jensen, B. Sellergren, G.R. Hutchison, A. Marcomini, V. Stone, In vitro assessment of engineered nanomaterials using a hepatocyte cell line: cytotoxicity, pro-inflammatory cytokines and functional markers, *Nanotoxicology*, 7 (2013) 301-313.
- [44] A. Kermanizadeh, B.K. Gaiser, M.B. Ward, V. Stone, Primary human hepatocytes versus hepatic cell line: assessing their suitability for in vitro nanotoxicology, *Nanotoxicology*, 7 (2013) 1255-1271.
- [45] A. Kermanizadeh, I. Gosens, L. MacCalman, H. Johnston, P.H. Danielsen, N.R. Jacobsen, A.G. Lenz, T. Fernandes, R.P. Schins, F.R. Cassee, H. Wallin, W. Kreyling, T. Stoeger, S. Loft, P. Moller, L. Tran, V. Stone, A Multilaboratory Toxicological Assessment of a Panel of 10 Engineered Nanomaterials to Human Health-ENPRA Project-The Highlights, Limitations, and Current and Future Challenges, *Journal of toxicology and environmental health. Part B, Critical reviews*, 19 (2016) 1-28.
- [46] K. Donaldson, V. Stone, P.J. Borm, L.A. Jimenez, P.S. Gilmour, R.P. Schins, A.M. Knaapen, I. Rahman, S.P. Faux, D.M. Brown, W. MacNee, Oxidative stress and calcium signaling in the adverse effects of environmental particles (PM10), *Free radical biology & medicine*, 34 (2003) 1369-1382.

- [47] A. Kermanizadeh, B.K. Gaiser, G.R. Hutchison, V. Stone, An in vitro liver model - assessing oxidative stress and genotoxicity following exposure of hepatocytes to a panel of engineered nanomaterials, *Particle and Fibre Toxicology*, 9 (2012).
- [48] M. Elsabahy, K.L. Wooley, Cytokines as biomarkers of nanoparticle immunotoxicity, *Chemical Society Reviews*, 42 (2013) 5552-5576.
- [49] D.M. Brown, C. Dickson, P. Duncan, F. Al-Attili, V. Stone, Interaction between nanoparticles and cytokine proteins: impact on protein and particle functionality, *Nanotechnology*, 21 (2010) 215104.
- [50] K. Unfried, C. Albrecht, L.-O. Klotz, A. Von Mikecz, S. Grether-Beck, R.P.F. Schins, Cellular responses to nanoparticles: Target structures and mechanisms, *Nanotoxicology*, 1 (2007) 52-71.
- [51] S.M. Moghimi, A.C. Hunter, C.M. Dadswell, S. Savay, C.R. Alving, J. Szebeni, Causative factors behind poloxamer 188 (Pluronic F68, Flocor™)-induced complement activation in human sera: A protective role against poloxamer-mediated complement activation by elevated serum lipoprotein levels, *Biochimica et Biophysica Acta (BBA) - Molecular Basis of Disease*, 1689 (2004) 103-113.
- [52] S.M. Moghimi, Modulation of Lymphatic Distribution of Subcutaneously Injected Poloxamer 407-Coated Nanospheres: the Effect of the Ethylene Oxide Chain Configuration, *Febs Letters*, 540 (2003) 241-244.
- [53] G. Sahay, E.V. Batrakova, A.V. Kabanov, Different Internalization Pathways of Polymeric Micelles and Unimers and Their Effects on Vesicular Transport, *Bioconjugate Chemistry*, 19 (2008) 2023-2029.
- [54] E.V. Batrakova, S. Li, A.M. Brynskikh, A.K. Sharma, Y. Li, M. Boska, N. Gong, R.L. Mosley, V.Y. Alakhov, H.E. Gendelman, A.V. Kabanov, Effects of pluronic and doxorubicin on drug uptake, cellular metabolism, apoptosis and tumor inhibition in animal models of MDR cancers, *Journal of Controlled Release*, 143 (2010) 290-301.
- [55] M. Redhead, G. Mantovani, S. Nawaz, P. Carbone, D.C. Gorecki, C. Alexander, C. Bosquillon, Relationship between the Affinity of PEO-PPO-PEO Block Copolymers for Biological Membranes and Their Cellular Effects, *Pharmaceutical Research*, 29 (2012) 1908-1918.
- [56] M.F. Clincke, E. Guedon, F.T. Yen, V. Ogier, O. Roitel, J.L. Goergen, Effect of surfactant pluronic F-68 on CHO cell growth, metabolism, production, and glycosylation of human recombinant IFN-gamma in mild operating conditions, *Biotechnol Prog*, 27 (2011) 181-190.
- [57] Y. Liu, H. Miyoshi, M. Nakamura, Nanomedicine for drug delivery and imaging: A promising avenue for cancer therapy and diagnosis using targeted functional nanoparticles, *International Journal of Cancer*, 120 (2007) 2527-2537.
- [58] J. Lovric, H.S. Bazzi, Y. Cuie, G.R.A. Fortin, F.M. Winnik, D. Maysinger, Differences in subcellular distribution and toxicity of green and red emitting CdTe quantum dots, *Journal of Molecular Medicine*, 83 (2005) 377-385.
- [59] R. Firdessa, T.A. Oelschlaeger, H. Moll, Identification of multiple cellular uptake pathways of polystyrene nanoparticles and factors affecting the uptake: Relevance for drug delivery systems, *European Journal of Cell Biology*, 93 (2014) 323-337.
- [60] H.J. Johnston, M. Semmler-Behnke, D.M. Brown, W. Kreyling, L. Tran, V. Stone, Evaluating the uptake and intracellular fate of polystyrene nanoparticles by primary and hepatocyte cell lines in vitro, *Toxicology and Applied Pharmacology*, 242 (2010) 66-78.
- [61] L. Shi, C. Tang, C. Yin, Glycyrrhizin-modified O-carboxymethyl chitosan nanoparticles as drug vehicles targeting hepatocellular carcinoma, *Biomaterials*, 33 (2012) 7594-7604.
- [62] M.J. Clift, C. Brandenberger, B. Rothen-Rutishauser, D.M. Brown, V. Stone, The uptake and intracellular fate of a series of different surface coated quantum dots in vitro, *Toxicology*, 286 (2011) 58-68.
- [63] H. Akita, K. Enoto, H. Tanaka, H. Harashima, Particle Tracking Analysis for the Intracellular Trafficking of Nanoparticles Modified with African Swine Fever Virus Protein p54-derived Peptide, *Molecular Therapy*, 21 (2013) 309-317.
- [64] M.S. Shive, J.M. Anderson, Biodegradation and biocompatibility of PLA and PLGA microspheres, *Adv Drug Deliv Rev*, 28 (1997) 5-24.

